

1956

Behavior of welded single-span frames under combined loading, *Welding Journal*, Vol. 35, p. 234-s, 1956, Reprint No. 107 (56-3)

C. G. Schilling

F. W. Schutz Jr.

L. S. Beedle

Follow this and additional works at: <http://preserve.lehigh.edu/engr-civil-environmental-fritz-lab-reports>

---

#### Recommended Citation

Schilling, C. G.; Schutz, F. W. Jr.; and Beedle, L. S., "Behavior of welded single-span frames under combined loading, *Welding Journal*, Vol. 35, p. 234-s, 1956, Reprint No. 107 (56-3)" (1956). *Fritz Laboratory Reports*. Paper 1413.  
<http://preserve.lehigh.edu/engr-civil-environmental-fritz-lab-reports/1413>

This Technical Report is brought to you for free and open access by the Civil and Environmental Engineering at Lehigh Preserve. It has been accepted for inclusion in Fritz Laboratory Reports by an authorized administrator of Lehigh Preserve. For more information, please contact [preserve@lehigh.edu](mailto:preserve@lehigh.edu).

Welded Continuous Frames and Their Components

Progress Report No. 17

BEHAVIOR OF WELDED SINGLE-SPAN FRAMES UNDER  
COMBINED LOADING

by

C. G. Schilling, F. W. Schutz, Jr., and L. S. Beedle

This work has been carried out as part of an investigation sponsored jointly by the Welding Research Council of the Engineering Foundation and the Navy Department with funds furnished by the following:

American Institute of Steel Construction  
American Iron and Steel Institute  
Office of Naval Research (Contract No. 39303)  
Bureau of Ships  
Bureau of Yards and Docks

Fritz Engineering Laboratory  
Department of Civil Engineering and Mechanics  
Lehigh University  
Bethlehem, Pennsylvania

March, 1955

Fritz Laboratory Report No. 205D.6

CONTENTS

	Page
I. INTRODUCTION . . . . .	1
1. Object and Scope of Investigation . . . . .	1
II. DESCRIPTION OF FRAMES AND TESTING APPARATUS . . . . .	3
2. Test Specimens . . . . .	3
3. Lateral Support System . . . . .	6
4. Loading System . . . . .	7
5. Determination of Experimental Moments . . . . .	8
6. Rotation Measurement . . . . .	10
7. Deflection Measurement . . . . .	10
8. Buckling Instrumentation . . . . .	10
9. Test Procedure . . . . .	11
III. THEORETICAL ANALYSIS . . . . .	14
10. Theoretical Loads and Moments . . . . .	14
11. Theoretical Deformations . . . . .	16
IV. RESULTS OF TESTS . . . . .	19
12. General Behavior . . . . .	19
13. Experimental Loads and Moments . . . . .	20
(a) Test Frame 3 . . . . .	20
(b) Test Frame 4 - Phase I . . . . .	23
(c) Test Frame 4 - Phase II . . . . .	25
(d) Plastic Design Working Loads . . . . .	27
14. Experimental Deflections . . . . .	29
15. Moment-Rotation Relationships . . . . .	31
(a) Beam to Column Connections . . . . .	31
(b) Beam Sections . . . . .	34
16. Plastic Buckling and Lateral Support . . . . .	37
(a) General . . . . .	37
(b) Frame 3 . . . . .	38
(c) Frame 4 . . . . .	42

CONTENTS  
(Continued)

	Page
V. SUMMARY . . . . .	44
VI. ACKNOWLEDGEMENTS . . . . .	48
REFERENCES . . . . .	49
NOMENCLATURE . . . . .	50
FIGURES	

S Y N O P S I S

The results of tests carried out on two full size portal frames are presented. These frames were of welded construction and had spans of 30 feet and column heights of 10 feet. The column bases were pin ended in one case and fixed in the other. The frames which were fabricated from 12WF36 shapes were subjected to simultaneous application of vertical and horizontal loads.

The behavior of the component parts of the frame (beams, columns, welded connections) as indicated by various measuring techniques are compared with computed values based on simple plastic theory. Attention was given to the problem of plastic instability.

The lateral forces required to restrain the frames to their original plane were measured and analyzed. These forces are of significance in both elastic and plastic design of such structures.

Information with regard to the action of fixed base frames under very high horizontal loads is presented.

## I. INTRODUCTION

### 1. OBJECT AND SCOPE OF INVESTIGATION

The tests reported herein are the third and fourth frame tests to be carried out at Lehigh University as part of the broad investigation titled "Welded Continuous Frames and Their Components". The frames were simple rectangular portals, one with pinned column bases and the other with fixed column bases. Both were fabricated from a 12WF36 steel section with a beam span of 30 ft. and 10 ft. column heights. The previous two frames tested in this program<sup>(1)\*</sup> were also rectangular portals with beam spans of 14 ft. and had columns 7 ft. high with pinned bases. The variable in the earlier frames was the size of section used; one was made from 8B13 shapes while the second was from 8WF40 shapes.

In contrast to the first and second test frames, which were subjected to vertical loads only, Test Frames 3 and 4 were subjected to a combination of horizontal and vertical loads.

In recent years an extensive study into the plastic behavior of steel structures has also been carried out at Cambridge University in England and tests of frames loaded under both vertical and horizontal loads have been reported.<sup>(2)</sup> The tests reported in these studies have been made on somewhat smaller frames fabricated from steel shapes rolled in England.

The main objective of the tests was to determine if the ultimate load-carrying capacity of such frames under combined

---

\* Numbers in parentheses indicate the reference number in the References.

loading could be predicted by simple plastic theory. In addition, valuable information regarding the lateral support required for such frames was ascertained as were the final modes of failure.

The frame with fixed column bases (Frame 4) demonstrated the large reserve strength such column fixity gives the frame to horizontal loads.

## II. DESCRIPTION OF FRAMES AND TEST APPARATUS

### 2. TEST SPECIMENS

The test specimens used are detailed in Fig. 1. Both were single bay rectangular rigid frames with beam spans of 30 ft. and column heights of 10 ft. The knees were of all welded construction and were Type 8B described in Ref. 3. Both frames were fabricated in the laboratory by welders and fitters whose regular jobs involve similar operations at the plant of a large steel fabricator.

If these frames were assumed to be from an imaginary building with an assumed vertical working load of 60 psf and design wind load of 20 psf, the resulting total vertical load would be nine times the total horizontal load. Such reasoning as this leads to the loading ratio which was maintained constant throughout Test 3 and during the first phase of Test 4. Loads were applied at the third points of both the beam and windward column. (The windward column herein refers to the column to which the horizontal loads were applied.)

The two frames differed only in the condition at the column bases. Frame 3 was pin-ended; that is, both column bases were mounted on knife edges. During the test the distance between knife edges was kept constant by means of tie rods. To simulate a fixed-ended condition, the column bases of Frame 4 were welded directly to a stiff base beam. Since the base beam was not infinitely stiff the columns' bases were not completely fixed.



This partial fixity had no effect on the theoretical ultimate load of the frame, although the frame's behavior in the elastic range was affected.

Both frames were fabricated from 12WF36 "as-rolled" steel sections. The dimensions were acquired with the aid of a micrometer and the actual properties of the section differed considerably from those given in the A.I.S.C. Steel Construction Manual.<sup>(4)</sup> A comparison of the actual and handbook properties is given in Table I. Both the actual section modulus,  $S_x$ , and plastic modulus,  $Z_x^*$ , were approximately 5% lower than the handbook values due largely to the discrepancy in flange thickness.

TABLE I: Section Dimensions and Properties

	Wgt. per ft. (lbs)	Area (in <sup>2</sup> )	Depth (in)	Flange		Web Thickness (in)	$I_x$ (in <sup>4</sup> )	$S_x$ (in <sup>3</sup> )	$Z_x$ (in <sup>3</sup> )
				Width (in)	Thickness (in)				
Handbook <sup>(4)</sup>	36	10.59	12.24	6.565	0.540	0.305	280.8	45.9	51.4
Actual	34.8	10.21	12.17	6.59	0.510	0.307	266.2	43.7	49.1
Variation*	-3.3%	-3.6%	-0.6%	+0.4%	-5.6%	+0.7%	-5.2%	-4.8%	-4.5%

\* % based on handbook value.

Values in table computed for T4 assumed applicable to both T3 and T4.

The mechanical properties of the steel used were determined by standard coupon tests (both tension and compression) conducted at a slow laboratory rate on coupons taken from four locations in the cross-section. A set of coupons was taken from the beam section used in fabricating each frame. The steel was ordered to meet the requirements of ASTM Designation A7-50T.

\*  $Z_x$  (plastic modulus) for symmetrical sections is 2 times the first moment of one half of the section about the neutral axis.

The laboratory coupon tests are summarized in Table II. In using these results to determine the yield moment ( $M_y = 1713$  kip in.) and the plastic moment ( $M_p = 1925$  kip in.) of the section the yield stress level of those coupons (tension and compression) located in the flanges were averaged and used as the yield stress. This average yield stress level was 39.2ksi, which is lower than the upper yield strength of 42.53 ksi given in the mill report (Table III), this value being determined from a coupon selected from the web.

If the plastic moment were computed on the basis of a weighted yield stress (both flange and web coupons being used) its value becomes 1943 kip in. This weighted value being 0.9 per cent larger than the plastic moment used in this report.

TABLE II: Physical Properties

X-Section Location	Coupon For Frame No.	Yield Stress Level $\sigma_y$ (ksi)	Ultimate Strength (ksi)	Modulus of Elasticity $E(x10^6$ ksi)	Strain-Hardening $\epsilon_{st}$ (in/in)
1	3	39.23	62.00	30.6	0.015
	4	39.08	62.23		0.017
	3	-38.06*		29.7	0.014
	4	-40.47			0.011
2	3	45.10	67.80	29.8	0.024
	4	44.66	66.56		0.018
	3	-45.15		29.7	0.014
	4	-47.20			0.013
3	3	39.70	62.20	29.8	0.018
	4	39.45	62.74		0.023
	3	-38.09		30.3	0.015
	4	-39.81			0.018
4	3	41.20	66.20	30.8	0.014
	4	38.66	62.85		0.019
	3	-38.49		30.9	0.013
	4	-38.35			0.009

Section Properties Used

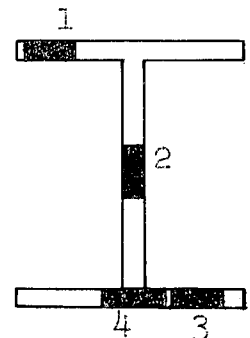
$\sigma_y - 39.2$  ksi

$M_y - 1713$  k"

$M_p - 1925$  k"

$E - 30.2 \times 10^3$  ksi

$EI - 80.39 \times 10^5$  k-in<sup>2</sup>



Coupon Location on Cross Section

\* "-" indicates compression test.

TABLE III: Mill Report on 12WF36

Chemical Composition in Per Cent	Mechanical Properties
C = 0.18	Yield Strength = 42,530 psi (upper yield)
Mn = 0.65	Ultimate Strength = 67,420 psi
P = 0.014	Elongation in 8 in. = 25.2 per cent
S = 0.038	Reduction in Area = 50.0 per cent

### 3. LATERAL SUPPORT SYSTEM

Past experience in testing of rigid frames into the plastic range had shown that adequate lateral support was essential if the theoretical ultimate load were to be attained. Therefore, the present test frames were provided with a lateral support system which might be equivalent to that used in actual building construction. In Test 3 this support was provided by 18 struts which held the frame in a plane about 10 ft. from the wall of the laboratory building. (See Fig. 2a) Four of these struts, which were located in elastic regions, carried very small forces in Frame 3 and, therefore, were not used in Test 4 which had a similar moment condition in the beam. The locations of lateral support struts are indicated by the small circles drawn on the flanges of the beam in Fig. 1.

In order to insure free vertical movement of the frame beam in its plane, the lateral support struts were fitted with flex bars at both ends. The lateral support at a typical beam section is shown in Fig. 3. Provisions were made to adjust the struts for large vertical deflections and the tests were planned

so that no horizontal adjustment was necessary. Electrical strain gages were attached to one of the flex bars of each lateral support strut so that the force in the individual struts could be ascertained at any time.

The lateral support system can be seen in the photograph of the general test arrangement shown in Fig. 2a.

#### 4. LOADING SYSTEM

In both frames the loads were applied by a self-contained system made up from the frame, a base beam and hydraulic jacks. Each jack was attached in series to an aluminum tube dynamometer for measuring the load applied. All loads were applied to the frame through horizontal pins located at the centroid of the beam and provided with transverse stiffener plates to help distribute the load to the section. The loading systems are shown in schematic form in Fig. 4.

In Frame 3 (see Fig. 4a) one jack was used for each of the two vertical loads, one for the horizontal loads, and one for the horizontal reaction at the column bases. This system of opposing horizontal jacks was used to adjust the longitudinal position of the frame so that the beam of the frame had no horizontal movement thereby simplifying the lateral support system. Each jack was connected directly to a hand-operated pump.

A slightly different loading system as shown schematically in Fig. 4b was used in Test 4. One jack was used for each load but the two vertical jacks were connected to a common pump. Similarly, the two horizontal jacks were connected to a second pump. This system expedited the test in the plastic range by automatically maintaining the loads applied by the two jacks approximately equal. The maximum difference in these loads was 2.1 per cent which occurred after ultimate load in Phase II. Reactions for the horizontal jacks were transferred to the base beam at points under the column bases. Reactions for the vertical jacks were also taken by the base beam so that the loading system was completely self-contained within the rectangular ring formed by the frame and the base beam. As in Test 3 the tops of the columns were fixed in space and the sidesway that occurred caused the base beam to move on rollers provided under it.

It should be pointed out that the loading systems used in these tests give the worst possible effect from the side loads since they require the beam to carry a maximum axial compression load. If, for instance, the horizontal load were applied in parts to both columns the beam would be subject to less axial compression load.

##### 5. DETERMINATION OF EXPERIMENTAL MOMENTS

Both frames were statically indeterminate, Frame 3 to the first degree, and Frame 4 to the third degree. It was, therefore, necessary to measure redundants in order to determine the experimental moments throughout the frames.

In Frame 3 it was sufficient to measure the horizontal force which existed in the column base tie rods. This was accomplished by means of SR-4 electrical strain gages mounted on aluminum links in the tie rods.

Six pairs of SR-4 electrical strain gages were attached to webs of the columns of Frame 4 in order to measure unit rotation at three points in each column. From the unit rotations, the moments were computed since the gages were mounted in regions expected to remain elastic. In the latter part of the test, the columns yielded at two of these points (one in each column) so that the moment could no longer be ascertained with certainty at those points. The four pairs of gages remaining, however, were more than enough to determine the moments throughout the frame. During the early part of the test when all gages could be used, the moments at the tops and bottoms of both columns were determined by using various combinations of gages. The maximum variation in the moments thus obtained was about 10%. This method of determining moments is discussed at some length in Ref. 1.

Once the redundants were determined the experimental moments throughout the frames were obtained by statics. These moments were corrected for frame distortions by using the measured frame deflections.

## 6. ROTATION MEASUREMENT

Measurements to determine the rotation occurring along a unit length of beam and across the knees of the frames were made by use of the rotation indicators described in Ref. 1. Such rotation indicators, four on Frame 3 and eleven on Frame 4, were located at points where plastic hinges formed. In order to get some indication of the extent of the plastic zone near the lee knee of Frame 4, a total of five indicators were located adjacent to the knee in the column and beam.

## 7. DEFLECTION MEASUREMENT

Ordinary surveying instruments were used to determine the deflected shape of both frames to within 1/50 of an inch. This precision was adequate in view of the fact that deflections in the order of 3 inches were experienced at ultimate load.

A transit (one for each column) was used to establish a fixed vertical plane from which the horizontal deflections of the column were measured. Similarly, an engineer's level was used to establish a fixed horizontal plane just above the frame from which the vertical deflections of the beam were measured. A single mechanical dial gage was used to measure the deflection at beam center as a check on the surveying instruments and for control during the test.

## 8. BUCKLING INSTRUMENTATION

Several types of instruments were used to detect lateral and local buckling. Mechanical dial gages were used to measure local movement of both the web and compression flange at

critical locations. In Frame 3 further indication of local flange buckling was given by pairs of SR-4 electrical strain gages mounted on opposite sides of the compression flange at critical points.

An indication of lateral buckling was obtained by measuring the lateral twist, or rotation, of the beam. In Frame 3 this was accomplished by transverse level bars (described in Ref. 1) mounted at three critical sections on the beam. This method was much more precise than necessary so a movable twist indicator was devised to measure the lateral twist at critical sections on the beam in Test 4.

## 9. TEST PROCEDURE

Both tests consisted of two parts: (1) check test of the frame in the elastic range and (2) main test carried out continuously through the elastic and plastic ranges to failure. The check tests were used to ascertain the behavior of both the testing apparatus and the frames.

Frame 3 was check-tested as a determinate structure by removing the tie rods connecting the column bases. In this condition the frame was loaded in three different ways: by vertical beam loads only, by horizontal column loads only, and by tie rod forces on the column bases. The resulting deflections at the beam center and column bases were measured. The maximum deviation of these deflections from the theoretical values was 6.5 per cent indicating that the testing apparatus and frame were



functioning satisfactorily. Frame 3 was also check-tested as an indeterminate structure. The force in the tie rods was measured and found to agree within 2 per cent with the theoretical value.

For Frame 4 such an elaborate check test was not possible since the specimen could not be reduced to a determinate structure. The beam center deflection, however, was measured and found to agree within 7 per cent of the theoretical value when the load was 12 kips in the vertical jacks. A further indication of the action of the frame is given by a comparison of the actual and theoretical moment diagrams in the elastic range shown in Fig. 5. Except at the column bases, these moments differed by approximately 5 per cent.

The main tests were carried out continuously until the lateral plastic buckling near the lee knee became excessively large causing rapid reductions in load-carrying capacity. The time required for the continuous tests was about 60 hours.

During the early stages of the tests, readings were taken on all measuring devices at frequent load intervals. No data were taken at a given load increment until the beam center deflection had stabilized; that is, with the loads on the frame held constant the increase in deflection with time became negligible.

As the applied loads approached the theoretical plastic ultimate load the time required for the deflection to stabilize increased rapidly. To reduce this stabilizing time a "deformation-

increment" criterion was adopted for the later part of the tests. Under this criterion a predetermined deformation increment was applied by means of the jacks. This deformation was then held constant while the loads decreased with time. Eventually, these loads remained practically constant and a set of data was taken.

For Frame 3 the horizontal loads were  $1/9$  of the vertical loads throughout the test. Test 4, however, consisted of two distinct phases. In the first phase, the frame was loaded with vertical and horizontal loads in a nine-to-one proportion until 97 per cent of the theoretical plastic ultimate load for this load condition was reached. In the second phase, the vertical loads were held constant at a value slightly less than the theoretical ultimate load and the horizontal loads were increased from zero to their ultimate value. Actually near the end of the test it was found impossible to keep the vertical loads constant without greatly increasing the vertical beam deflections. At this stage the vertical loads were allowed to decrease slightly.

In effect, Test 4 was two tests -- one in which the vertical loads had a dominant effect, the other in which the horizontal loads were more significant. The first case wherein the vertical loads were maintained at values 9 times the horizontal load is referred to as Test 4 - Phase I or Test 4(I); in that part of the test in which the vertical load was held constant as the horizontal load was increased is referred to as Test 4 - Phase II or Test 4(II).

### III. THEORETICAL ANALYSIS

#### 10. THEORETICAL LOADS AND MOMENTS

The results of the theoretical analysis of the frames are summarized in Figs. 6 and 7. In the elastic range the structures were analyzed by ordinary elastic methods for indeterminate structures. Since the base beam in Frame 4 was not infinitely rigid, its actual rigidity was taken into account in the elastic analysis. The structure was analyzed as a closed ring composed of the frame itself and the base beam. It must be emphasized, however, that this base beam flexibility had no effect on the theoretical ultimate load found by simple plastic analysis so long as the base beam remained elastic. Methods of simple plastic analysis by which the ultimate loads of frames such as these may be predicted have been described. (5 to 7)

TABLE IV: Critical Loads From Theoretical Analysis

Load	Frame 3 Kips	Frame 4	
		Phase I Kips	Phase II Kips
P (Yield)*	23.7	26.2	18.7
Q (Yield)*	2.63	2.91	18.7
P (Ultimate)	29.9	32.1	32.1
Q (Ultimate)	3.32	3.57	32.1

\*Load at which bending stresses alone are equal to yield stress of material (39.2 ksi). If axial stress were added loads  $P_y$  and  $Q_y$  would be lower.

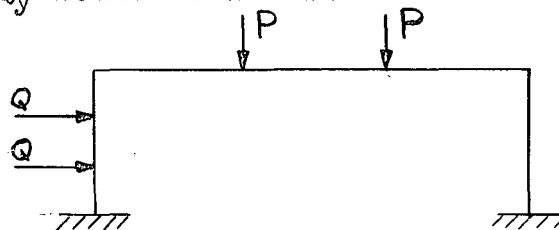


Table IV gives the applied loads at the theoretical first yield ( $P_y$  and  $Q_y$ ) and at the theoretical ultimate load condition ( $P_p$  and  $Q_p$ ). They are based on the actual physical properties of the section,  $M_y = 1713$  kip in. and  $M_p = 1925$  kip in. A study of this table reveals that the theoretical ultimate strength given by plastic analysis is 1.26 times as great as the conventionally accepted maximum strength (load at first yield) for Frame 3 and 1.22 times as great for Frame 4 (I). Another point of interest is the capacity of Frame 4 to withstand very high horizontal loads. In Phase II of the test the horizontal ultimate loads are as large as the vertical ultimate loads. The plastic analysis ultimate load for the condition of equal horizontal and vertical load (Frame 4, (II)) is 1.72 times as great as for the first yield ultimate concept. It should be pointed out that the first yield loads listed in Table IV are based on stresses caused by bending moments alone. If axial forces were also considered (as they generally are in elastic analysis) the first yield loads would be somewhat lower.

The ultimate loads were obtained by using simple plastic theory. The sequence of the formation of plastic hinges is given by the circled numbers in Figs. 6 and 7. The first four hinges shown for Frame 4 in Fig. 7 were required in order that the theoretical ultimate load in Phase I could be reached. Hinges 1 and 3 remained hinges in Phase II. In addition to these hinges, two others (5 and 6) were necessary in order that an ultimate load could be reached in Phase II. In Phase II, hinges 2 and 4 behaved elastically because the moment at these hinges produced by the horizontal loads was opposite to the plastic moments produced by the vertical loads in Phase I.

The base beam used in Test 4 was not infinitely stiff, therefore its true value of  $E$  and  $I$  were used in the theoretical computations whose results are summarized above. It is of interest to note that while this lack of complete fixity at the base of the columns in Frame 4 does affect the moment distribution in the frame in Phase I it does not affect the total load-carrying capacity of the frame. The ultimate load ( $P = 32.1$  kips) moment diagram shown in Fig. 7 (and repeated in Fig. 8) for Frame 4 (I) takes into account the base beam flexibility. If the base beam were infinitely stiff or rigid the theoretical ultimate load ( $P = 32.1$  kips) moment diagram would be altered. A comparison of the two conditions is given in Fig. 8.

#### 11. THEORETICAL DEFORMATIONS

In order to check the actual behavior of the frames against the theoretical behavior, some measurable quantity other than applied forces should be predicted by theoretical means. One such quantity chosen for the present tests is the deflection of the center of the beam.

While the frame is in the elastic range the beam centerline deflection may be determined by ordinary elastic analysis. However, such analysis assumes the frame to be formed from members having lengths given by the centerline dimensions of the frame. This assumption leads to an answer which is approximately correct but it can be improved upon by taking into account the fact that the particular knees of the frame rotate more than the equivalent length of plain beam. A rational method of predicting such difference in rotation is given in Ref. 2.

In the case of Frame 3, this procedure led to a beam center deflection of 1.79 in. at yield load instead of 1.74 in. This increase is so small that the effect was ignored in the computations for Frame 4.

Approximate values for deflections of the frames may be determined just as the ultimate load is reached by a very simple method described by Symonds and Neal<sup>(5)</sup> and Yang et al<sup>(8)</sup>. This method assumes that yielding is concentrated at the plastic hinges and that these hinges are free to rotate under the constant moment,  $M_p$ , other parts of the frame remaining elastic. Just as the last plastic hinges is formed the slope at either side of the hinge must be equal. Using these assumptions and the slope-deflection equations, one may find the deflected shape of the structure. For Frame 3 this gives an estimated beam center deflection of 2.82 in. at ultimate load. It seems reasonable that the actual deflection should be larger than 2.82 in. since yielding is spread out over lengths of the beam and not concentrated at the hinges as assumed in the analysis. This would be particularly true in the present case since the entire center third of the beam is withstanding a moment greater than  $M_y$  when the ultimate load is reached.

The deflection computations discussed above for Frame 3 allow one to draw the theoretical load-deflection curve shown on Fig. 9. Similar computations result in the theoretical load deflection curve shown in Fig. 10 for Frame 4 where the beam center deflection at ultimate load was computed to be 3.64 in. Again it should be pointed out that for Frame 4 as well as for Frame 3 the actual moment diagram violates the assumption,

"plastic hinges are concentrated at points" made in the deflection computation. Figure 7 shows that the entire middle third of the beam in Frame 4 is under the theoretical plastic hinge moment at the ultimate load condition. This condition assures one that the actual deflection will be considerably larger than the computed value. In the case of structures having moments that continuously vary, there should be much closer agreement between theoretical and experimental deflection values.

In any case, the fact that the actual deflections at maximum load are somewhat larger than the theoretical values is not critical since at plastic design working loads the agreement between theory and experiment is excellent.

#### IV. RESULTS OF TESTS

##### 12. GENERAL BEHAVIOR

The present test frames and test apparatus behaved as well as was expected in all respects. It is believed that the results indicate the performance that might be expected from an actual building frame where the proper consideration is given the lateral support system. At the same time, a lateral support system capable of providing the support given the test frames might not be impractical; in fact, even better support is often given the frames of elastically-designed structures (such as concrete floor slabs, etc.).

The frames carried the predicted yield loads and approached the theoretical ultimate load very closely. In addition, both frames showed an ability to carry loads very near the predicted ultimate load even when the deflections were double those at the time the ultimate load was first reached. This characteristic which is clearly seen in Figures 9 and 10 demonstrates the large energy absorbing capacity of structural steel rigid frames when loaded into the plastic state.

Final failure for Frame 3 was eventually brought about when the lee column buckled laterally just below the beam-column connection. This buckling occurred in a region that was fully plastic and was a clear case of plastic instability. Other "minor" cases of plastic instability took place but were prevented from progressing to such an extent as to be the cause of the frame failure. The ability of the frame to survive these



earlier cases of plastic instability was undoubtedly due to the effective lateral support system.

Plastic instability also brought about the final failure of Frame 4. For this frame the lateral buckle occurred in the beam in a region immediately adjacent to the connection of the lee column.

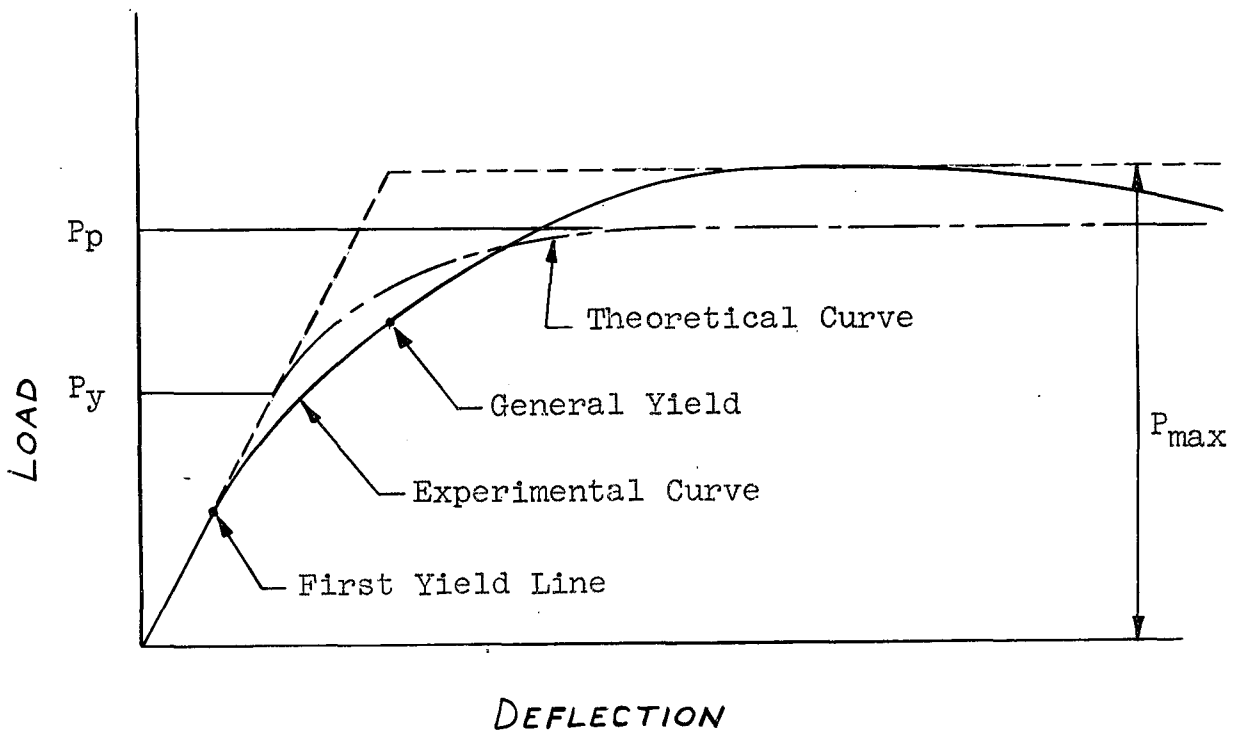
### 13. EXPERIMENTAL LOADS AND MOMENTS

#### (a) Test Frame 3:

The results of Test 3 with regards to load-carrying capacity are shown in one form in Figure 9 where the beam center deflection and the sidesway are plotted against the vertical load. The experimental load for this frame was 29.7 kips which is 99.3 percent of the theoretically computed load of 29.9 kips. Table V shows the ratios of certain test loads to the theoretically computed equivalents. For Frame 3 the first observed yield (aside from very minute local yield) was observed at 15.9 kips of vertical load as compared to computed yield load of 23.7 kips. (This computation for yield load neglected the effect of axial load). The tendency of a real frame to yield at low loads is discernible in Figure 9, in which inelastic action commenced at a vertical load of about 10 kips.

TABLE V: Strength Comparison

Frame No.		Yield Strength		Maximum Strength	
		First Yield Line kips	General Yield kips	Elastic Analysis Comparison kips	Plastic Analysis Comparison kips
1 (8WF40)	Observed	22.0	40.4	52.4	52.4
	Computed	39.4	39.4	39.4	47.7
	Ratio	0.56	1.05	1.33	1.10
2 (8B13)	Observed	5.5		18.0	18.0
	Computed	13.1		13.1	18.1
	Ratio	0.42		1.37	0.99
3 (12WF36)	Observed	15.9	25.3	29.7	29.7
	Computed	23.7	23.7	23.7	29.9
	Ratio	0.68	0.68	1.26	0.99
4 Phase I (12WF36)	Observed	19.0	26.0	31.0	31.0
	Computed	26.2	26.2	26.2	32.1
	Ratio	0.34	0.99	1.18	0.97
5 Phase II (12WF36)	Observed	--	26.7	30.5	30.5
	Computed	18.7	18.7	18.7	32.1
	Ratio	--	1.43	1.63	0.95



It is of interest to note what the allowable load for Frame 3 would be under present A.I.S.C. specifications<sup>(4)</sup> when section 12 (Combined Stresses) is applied. If only the vertical loads were placed on the frame, the A.I.S.C. allowable load would be 12.2 kips. The case of vertical and horizontal (wind) loads would not control since when this case is considered the allowable stress is increased 33 percent and the allowable load becomes 14.8 kips for Frame 3. Thus the real elastic design safety factor against the actual ultimate load for Frame 3 was 2.44 ( $29.7 \div 12.2$ ). This value compares with a value of 1.96 which would be obtained by dividing the actual yield stress by the allowable stress ( $39.2 \div 20$ ).

During the loading sequence of Frame 3 a complete set of data was taken when the vertical loads reached 12.0 kips each. The resulting moment diagram for this load condition is shown in Figure 11. The maximum stress due to bending at this load was 19.44 ksi at the lee knee of the frame. The moments shown in this diagram (the solid line in Figure 11) are close to those which would occur in this frame if it were designed elastically by A.I.S.C. specifications<sup>(4)</sup>.

When the elastic design moment diagram discussed above is compared with the two ultimate load moment diagrams in Figure 11 the reserve strength of the frame is further illustrated. The ultimate load moment diagram (Figure 11) computed by use of simple plastic theory<sup>(5)</sup> shows extremely close agreement with the one derived from measured reactions and statics in the actual frame.

(b) Test Frame 4 - Phase I:

As has been described before (Articles 9 and 10) Frame 4 was subjected to two separate loading conditions. Under each loading condition the frame was loaded to its ultimate capacity. During Phase I of Test 4 the loading condition was identical with Frame 3, (the vertical loads being nine times larger than the horizontal loads). The plastic mechanism which formed, however, was confined to the beam and sidesway was held to a minimum as can be seen from Figure 10. The sidesway at the ultimate load (Load 22) was only about 0.4 in. compared to a value of 1.6 in. for Frame 3 at its ultimate load.

Table V and Figure 10 give comparisons of the experimental and theoretical behavior of Frame 4(I). The ultimate load reached in the test was 31.0 kips which is 97 percent of the ultimate load of 32.1 kips computed by plastic theory. It should be pointed out, however, that this phase of the test was discontinued arbitrarily at this point in order that Phase II could be undertaken before the frame became too seriously deformed. The subsequent behavior of certain critical parts of the frame in Phase II indicates that the ultimate load had not been reached at Load 22 (Vertical load = 31.0 kips.) and had the test been continued under the Phase I loading ratio, it would have carried vertical loads as high as about 33.4 kips which would have been 104 percent of the theoretical ultimate load.

The first significant yielding occurred in Frame 4 during Phase I at a load of 9.0 kips or at only 34 percent of the computed yield load (yield load being computed neglecting

the effect of axial loads). The elastic design load for Frame 4(I) when the AISC interaction formula is used would be 12.6 kips for vertical loads only and 16.3 kips for vertical loads and horizontal wind loads. Thus the vertical loads would control an elastic design. Therefore, the demonstrated safety factor for the frame during Phase I was 2.46 ( $31.0 \div 12.6$ ) and might have been higher if the test had been continued. The difference between the safety factors of 2.46 and 1.96 (yield stress, 39.2, divided by allowable stress, 20.0) is due to the equalization of the moment diagram as plastic hinges are formed and to the shape factor (full plastic moment divided by yield moment). For the particular WF section (12WF36) used in these tests the shape factor is 1.12 ( $1925 \div 1713$ ).

Figure 12 shows moment diagrams for Frame 4(I). The experimental moments observed at a load ( $P = 12.0$  kips) near the elastic design load is shown. The other two diagrams give a comparison of the experimental and computed moments at the ultimate load condition. There appears to be a large discrepancy between these two diagrams. (In spite of this, the experimental and theoretical ultimate loads are in close agreement.) The explanation for the discrepancy in moment diagrams is that in attaching the frame column bases to the base beam, the column bases were forced apart in order to meet the required dimensions, thereby introducing a state of "locked-up" moments approximately equal to those shown in Figure 13(a). The exact horizontal force exerted at the bases of the columns when the frame was attached is not known, but by taking the average of the errors in

experimental moments at the knees at ultimate load in Figure 12 the force of 1.72 kips shown in Figure 13(a) was obtained. Such a value is well within the realm of reason.

The electrical strain gages used for moment determination in Frame 4 were mounted after these "locked-up" moments had been induced. Therefore the moments indicated by these gages were always in error by an amount equal to the "locked-up" moments. When the "locked-up" moments shown in Figure 13(a) are added to the experimental ultimate load moments shown in Figure 12 the more nearly correct experimental moment diagram shown in Figure 13(b) is obtained.

It should be emphasized that the "locked-up" moments discussed above have no effect on the ultimate load carrying capacity when plastic action is relied on. In a like manner the true ultimate load carrying capacities of rigid steel frames are not affected by such things as foundation settlement and rotation, small fabrication errors in dimensions of parts, or temperature changes. According to conventional (elastic) concepts, such factors are of significant influence. However, more often than coping with them, they are ignored in present design procedures; knowingly or not, plastic action is depended upon to assure the successful operation of the structure.

#### (c) Test Frame 4 - Phase II

During Phase II of Test 4 the vertical loads were held as nearly constant at 31.0 kips as possible while the horizontal loads were increased. This increase in horizontal

load was possible since the plastic mechanism developed in Phase I was local -- that is, confined to the beam. The columns were still stable structural elements since no plastic hinges had formed at their bases. In reviewing the behavior of the frame during Phase II, it should be remembered that the beam had already become a mechanism at the end of Phase I with a deflection at the center of the beam of 5.8 in. The frame undoubtedly would have withstood a larger ultimate load had the vertical and horizontal loads been equal from the outset in the test of an undeformed frame.

Despite the severe deformation of the frame at the start of Phase II, Frame 4 was able to withstand horizontal loads of 30.5 kips which is 95 percent of the theoretical plastic analysis load of 32.1 kips. (See Table V and Figure 10). This load was reached at about the same time the available stroke on the tension loading jacks was used up. As is indicated on Figure 10 the frame had to be unloaded at this point (Load No. 42) in order to shorten the loading rods. Once this was done the frame was never able to carry again its previous high load.

The advantage of fixed-based columns for certain loading conditions is clearly illustrated by the fact that Frame 4 in Phase II withstood horizontal loads 9.24 times larger than supported by Frame 3 with a resulting sidesway of 2.4 in. compared to a value of 1.6 in. in Frame 3.

If one were to assume the horizontal loads applied to Frame 4 in Phase II were not wind loads (such a high ratio of wind load to vertical load is unlikely) the elastic design

load would be 9.65 kips. Thus the present frame despite its adverse strain history was able to demonstrate a safety factor of 3.16. The factor would have been somewhat higher, perhaps as much as 3.4, if the frame had been loaded in its virgin condition with equal vertical and horizontal loads.

A comparison is made in Figure 14 between the experimentally and theoretically determined moments at ultimate load in Frame 4(II). The experimental moments here plotted are subject to the same errors brought on by the "locked-up" moments described for Phase I. The experimental moments at ultimate, Phase II, corrected for the "locked-up" moments given in Figure 13(a) are shown in Figure 15. Discrepancies between the experimental moments and the theoretical values in Figure 15 are partly due to the adverse strain history of the frame in Phase II and the fact that both corner connections are capable of carrying moments higher than the plastic hinge moment of a plain beam section. Another factor to be discussed later was the fact that part of the middle third of the beam had buckled laterally during Phase II, thereby reducing the moment carrying capacity of that beam section and forcing the corner connections to carrying increased moments.

#### (d) Plastic Design Working Loads

The preceding sections discussing the load-carrying capacities of Frames 3 and 4 have pointed out the large reserve in strength these frames have demonstrated over and above the commonly accepted elastic design loads. This characteristic



is due to the continuity existing in the frame brought about by welding such that the full plastic strength was developed. A new concept of design in structural steel, called "plastic design", makes use of this reserve strength which has herein been demonstrated. Much progress has been made in Great Britain in this area where actual structures have been built which were designed by use of plastic analysis<sup>(9)</sup>. One advantage of plastic design is the fact that all structures so designed will have a uniform and rational factor of safety regardless of the degree to which the structure is indeterminate in the elastic state.

Figure 16 illustrates how the five tests carried out at Lehigh University under the present program would have a uniform factor of safety under the plastic design concept. For purposes of discussion a load factor of safety of 1.75 against the theoretical ultimate load has been chosen. Thus the plastic design working load would be 57 percent of the theoretical ultimate load for all frames and for the typical simple beam as well. The bar chart (Figure 16) shows that the conventional elastic design procedures would use varying amounts of the ultimate load capacities (from 30 percent to 57 percent). It will be noted that elastic design and plastic design would permit the same working load for the case of a simple beam. Therefore, the rigid frame proportioned by plastic design would enjoy the same real safety factor as do present elastically-designed simple beams.

Further, Figure 16 shows that no part of the frames tested would have reached a condition of general yielding at the plastic design working load. Indeed, only the most unusual frame would be called upon to withstand general yielding at working loads as determined by plastic design using a reasonable load factor of safety.

The bar indicating the behavior of Frame 4(I) in Figure 16 is topped by an arrow showing the ratio of test load to theoretical that would be expected had the loading Phase I been continued. This expected load was based on subsequent behavior of parts of the frame in Phase II. It should also be remembered that Phase II of Test 4 was started after the frame had undergone large deformations which undoubtedly adversely affected its ultimate load-carrying capacity.

#### 14. EXPERIMENTAL DEFLECTIONS

The deflection characteristics of Frames 3 and 4 are shown in Figures 9 and 10, where the deflections at the center of the beam span and the sidesway of the tops of the columns are plotted versus the loads applied. In general, the deflections measured were as predicted by theory. Both frames showed beam deflections which deviated from the theoretical curves well before the theoretical yield load was reached. However, this deviation did not start to increase at a large rate until after the theoretical yield load,  $P_y$ , had been exceeded. Thereafter, it was "controlled" until the observed maximum load was reached.

Another presentation of the manner in which the structures deformed is given in Figure 17, where the deflected shapes of the frames at several load conditions are shown. The first deflection curve drawn in Figure 17(a) shows the shape of Frame 3 when the vertical load in each jack was 12 kips. This load produced a moment of 852 in. kips at the lee knee and a unit stress of 19,440 psi due to bending stress. It is approximately equal, then, to a normal design load by conventional elastic methods if direct stress is neglected.

The second deflected shape of Figure 17(a) is drawn for a vertical load of 18 kips. This load is near the allowable load that might be used in a plastic design using a load factor of safety of 1.75. At this load the frame is still well within the elastic limit. The maximum deflection at this load was 1.47 times the maximum deflection at the conventional elastic design load.

The shape of the frame at ultimate load, 29.7 kips, is given by the third curve on Figure 17(a). The curve showing the largest deflection is for the last load put on the structure and is therefore the greatest deformation that occurred. The load at this time was 26.5 kips. The lee column had already buckled laterally at this stage of the test. Despite the column failure and the large distortions, the frame was still carrying 89 percent of the ultimate, 221 percent of the normal elastic design load, and 151 percent of a "possible" plastic design load which uses a safety factor of 1.75 against the ultimate load.

The two curves showing the smaller deflections in Figure 17(b) were drawn for vertical loads of 12 and 18 kips on Frame 4(I). These loads correspond roughly to working loads that would be allowed on the frame by elastic design and plastic design, respectively.

The third deflected shape shows the condition of Frame 4 at its ultimate load ( $P = 31.0$  kips) at the end of Phase I. The fourth, and last, curve is drawn for the ultimate load ( $Q = 30.5$  kips) condition in Phase II.

The deflections shown in both parts of Figure 17 are exaggerated for clarity. The scale for plotting deflections is 4.8 times larger than the scale to which the frame center line is drawn.

## 15. MOMENT-ROTATION RELATIONSHIPS

### (a) Beam to Column Connections

Since one of the basic requirements of a material and a section to be used in a structure designed by plastic analysis is the ability to form plastic hinges, it is of interest to study moment-rotation relationships of certain critical parts of the present frames.

One such critical part is the beam to column connection or the knee of the portal frame. The knee should be able to withstand the full plastic moment of the beam section through large rotations. The connections used were chosen for the present frames because previous tests<sup>(3)</sup> at Lehigh University assured their good performance. The connections used in the present frames were designated as Type "8B" in Reference 3.

At no time during the tests did any knee show signs that it had a smaller moment capacity than the beam section. There was no local crippling of any parts even though yielding of the material was widespread in some of the knees.

The photographs in Figure 18 are close-up views of the lee knee of Frame 3. This knee was subject to large rotations and high moments. The photograph in Figure 18(a) was taken just after the frame had reached its ultimate load. It will be noted that at this load yielding (indicated by the dark bands in the white wash coating) had extended beyond the connection proper into both the beam and column. The condition of the same connection at the end of the test is shown in Figure 18(b). In this photograph the shift of the neutral axis in the column due to the axial load is clearly illustrated by the yield bands. On the other hand, the yielded zones in the beam just outside the connection are nearly symmetrical. The fact that the zone of yielded material extends further into the column than the beam can be attributed to two conditions. First, the high axial load stresses in the column are additive to the bending stresses. Secondly, the moment gradient is much steeper in the beam than in the column (see Figure 6, ultimate load moment diagram). The rotations of the connections at which the photographs in Figure 18 were taken are indicated on Figure 19.

The moment-rotation curves for both knees of Frame 3 are shown in Figure 19. At no time during the test did the knees show signs that they had smaller moment capacity than the beam section. There was no local crippling of any part even though yielding of the material was widespread in the knee at

the lee column. The knee showed the capacity to carry the full plastic moment of the beam section through large rotations. The moments at the intersection of beam and column center lines based on measured reactions and measured frame deflections are used in the plotting of one set of curves (drawn with solid lines) shown in Figure 19. The second curve for the lee knee (dashed line) was plotted with moments found when the deflection of the frame was neglected. The difference in the curves becomes significant only at very large rotations, well after the ultimate load had been reached.

The knee at the windward column was never called upon to carry a moment equal to the theoretical yield moment; nevertheless, the moment-rotation curve for this knee is not a straight line, and when the frame was unloaded the knee had taken on a small amount of permanent set, indicating inelastic action. As can be seen in Figure 19 the two knees of Frame 3 behaved in almost identical fashion at equal moment levels.

The moment rotation curves for Frame 4 shown in Figure 20 are plotted on the basis of experimental moments corrected for the frame deformations. These moments, however, have not been corrected for the suspected "locked-up" moments discussed in connection with Figure 13. These curves are in very close agreement with those of Figure 19, if the error in moment due to the initial "locked-up" moments is taken into account. One point worthy of note is the fact that the windward knee had virtually no increase in rotation during the interval between ultimate load - Phase I (Load 22) and ultimate load - Phase II

(Load 42) while the rotation in the lee knee more than doubled. This behavior is in complete agreement with the plastic theory for Phase II where the horizontal loads were increased while the vertical loads were held constant.

Another point of interest in Figure 20 is the unloading of the lee knee that occurred after the ultimate load had been reached in Phase II. This unloading occurred as the connection and the adjacent beam began to buckle laterally. Despite this unloading of the buckled lee knee the loads on the frame did not reduce at the same rate, in fact the vertical loads held about constant while the horizontal loads were increased (see Figure 10). This action was possible because of the ability of the windward knee to withstand increased moment and rotation as shown by the later part of its moment-rotation curve.

#### (b) Beam Sections

The moment-unit rotation relationships for two locations in Frame 3 are shown in Figure 21. The theoretical curves shown in this figure are simplified by showing only the two straight line portions of the true theoretical moment-unit rotation curve. The values of the moments plotted here were determined from measured reactions and were corrected for frame deformations. The curve for Location 1 in the lee column shows that the full plastic moment was never reached at this point in the frame; nevertheless, what appears to be plastic hinge action was started at the ultimate load condition when the moment at the section was 94 percent of the theoretical plastic moment. As the rotation increased rapidly after the ultimate load had

been reached, the moment increased slightly to 97 percent of the  $M_p$  value but only after the rotation was about five times greater than it was at the ultimate load. This reduced plastic moment can be attributed in part to the axial load in the column.

It should be pointed out that the moment-carrying capacity at Location 1, Figure 21, was not appreciably decreased until the column buckled laterally. The rotation when column buckling occurred was about 5.3 times as large as the rotation when the ultimate load was reached.

The second curve in Figure 21 shows the moment-unit rotation relationship found by the rotation indicator mounted on the frame near the theoretical location of the second plastic hinge (Location 2). This curve is very similar to the first curve except for the drop in the moment which occurs just after the ultimate load was reached. This reduction can be explained by the fact that the beam tried to buckle laterally in this region soon after the maximum load was attained. This buckle could be observed by eye shortly after the ultimate was reached, but its effect was undoubtedly indicated much sooner by the drop in moment at this section and by the drop in applied load seen on Figure 9. The detrimental effect of this lateral buckling action was finally overcome as the lateral supports in the region were sufficient to prevent increased lateral movement. After this sudden drop, the moment at the section increased again and exceeded the peak value which occurred at the ultimate load condition.



Moment-unit rotation curves for two beam sections in Frame 4 are shown in Figure 22. As in Figure 21, the theoretical curve is "idealized" by two straight lines. In the first curve, the moment 6 inches from the base of the windward column is plotted versus the average unit rotation of the lower 12 inches of the column. This area of the frame was still elastic at the ultimate load condition for Phase I, but became plastic as the horizontal loads were increased in Phase II. The experimentally determined moments at the base of the windward column are approximately correct since the "locked-up" moments shown in Figure 13(a) are zero there. Evidence of strain hardening is shown by the last portion of the curve.

The second curve in Figure 22 shows the moment-unit rotation relationship for a section of the beam 8 inches from the windward vertical load in Frame 4. The rotation indicator was mounted in an area where the last plastic hinge formed in Phase I (see Figure 7) since the third and fourth hinges formed simultaneously in Phase I. This explains the small rotation experienced by the beam at the ultimate load, Phase I. This curve is characterized by a sudden drop in moment just after ultimate load, Phase I, much like that shown in the corresponding curve in Figure 21. Again, lateral buckling of the beam in the center third is the explanation.

The moments used in plotting the second curve in Figure 22 were those computed from experimental data with corrections made for frame deflection. However, they were not corrected for the probable "locked-up" moments described in Figure 13. If this correction had been made, the maximum moment

carried at this point of the frame would have been 96.5 percent of its theoretical plastic moment,  $M_p$ . This percentage compared very favorably with a value of 97 percent shown by the corresponding beam section in Frame 3.

## 16. PLASTIC BUCKLING AND LATERAL SUPPORT

### (a) General

The present frames illustrated clearly the fact that the final failure of continuous rigid frames is usually brought about by instability of some part or parts of the frame. The proportions of most frames and rolled sections are such that this instability does not develop in the elastic range. Once the steel member has yielded, however, the possibility of this phenomenon occurring is increased many times. Current investigations at Lehigh University are making extensive studies into the field of plastic instability of rolled steel sections with the aim that adequate protection against premature buckling can be assured.

One way to prevent instability failure is to support the frame transversely. The location and strength of the lateral support system for a frame is of primary importance. At the same time the width-to-thickness ratio of the elements of the sections is also very important, since such elements may suffer from local buckling or crippling and thus bring about premature failure of the frame.

The proportions of the 12WF36 section used in the present tests are such that local buckling prior to strain

hardening would not occur. (See Ref. 10) Indeed, this characteristic was one reason for choosing the section for the tests. Studies now under way at Lehigh University indicate that if a section does not buckle locally before it reaches strain hardening it will have adequate rotation capacity for plastic design purposes provided it does not suffer from lateral (torsional) buckling.

(b) Frame 3

Frame 3 suffered from buckling in three regions. All three zones affected were in a plastic state when the buckling occurred. The first evidence of instability was observed by eye after the ultimate load had been reached and took the form of a lateral displacement of the compression flange of the beam near the second plastic hinge. The effect of this lateral buckle has already been discussed with regard to the drop in moment capacity of the beam in the region where the buckle occurred (See Figure 21). This buckle took the form of a wave about 3 ft. long, but further displacement was controlled by the lateral supports which were attached to the beam at the intersection of web and flange. (The locations of these supports along the beam are indicated by the circles in Figure 1(a).)

At the same time that the lateral buckle was observed in the beam, another type of instability was observed in the bottom flange of the beam at the lee knee in the form of flange crippling. The buckle occurred only in one-half of the flange with a wave length of about 3 or 4 inches. The center of the wave was about 4 in. from the intersection of beam and column. The yielded zone in which this buckle occurred can be seen in Figure 18(a). The buckle could be seen on the beam at the time

the photograph was taken, but it is not easily discernible in the photograph. Though this buckle was observed soon after ultimate load had been reached, it did not appear to hinder the performance of the frame in any way. Certainly it did not have the weakening effect of the lateral buckle which occurred in the middle third of the beam.

In this second case of instability, as in the first, good lateral support was near at hand and may have prevented damage that might have developed had it not been there.

The third case of instability came when the unsupported compression flange of the lee column buckled laterally and the frame finally collapsed (See "LB" in Figure 9). This buckle showed some early signs of developing in the form of an unequal yield pattern on the flange but apparently was held in check for some time by the lateral support attached to the compression flange at the intersection of beam and column. However, when the deflection at the center of the beam had reached a value of about 2.3 times its value at ultimate load, there was a distinct and rapid increase in the size of the buckle wave and a corresponding sudden drop in load. Despite this buckling, the frame supported 87.2 percent of its ultimate load but further straining produced rapidly decreasing load capacity. Just before the lee column buckled the load was 95.3 percent of the ultimate load.

The buckle in the lee column is shown after completion of the test in Figure 23. The photograph, which was taken from the inside of the frame looking out shows clearly the lateral-torsional buckling type of failure characterized by the lateral displacement of the compression flange.

the photograph was taken, but it is not easily discernible in the photograph. Though this buckle was observed soon after ultimate load had been reached, it did not appear to hinder the performance of the frame in any way. Certainly it did not have the weakening effect of the lateral buckle which occurred in the middle third of the beam.

In this second case of instability, as in the first, good lateral support was near at hand and may have prevented damage that might have developed had it not been there.

The third case of instability came when the unsupported compression flange of the lee column buckled laterally and the frame finally collapsed (See "LB" in Figure 9). This buckle showed some early signs of developing in the form of an unequal yield pattern on the flange but apparently was held in check for some time by the lateral support attached to the compression flange at the intersection of beam and column. However, when the deflection at the center of the beam had reached a value of about 2.3 times its value at ultimate load, there was a distinct and rapid increase in the size of the buckle wave and a corresponding sudden drop in load. Despite this buckling, the frame supported 87.2 percent of its ultimate load but further straining produced rapidly decreasing load capacity. Just before the lee column buckled the load was 95.3 percent of the ultimate load.

The buckle in the lee column is shown after completion of the test in Figure 23. The photograph, which was taken from the inside of the frame looking out shows clearly the lateral-torsional buckling type of failure characterized by the lateral displacement of the compression flange.

It has already been pointed out that earlier failure of the frame was undoubtedly prevented by the effective lateral support furnished for the test frame. A study of the forces that were measured in the lateral supports showed that the frame required negligible lateral support in the elastic range, but as zones of yielding in the frame formed, the lateral support system was called upon to carry larger and larger loads. Those lateral support struts located at the theoretical plastic hinges were called upon to carry the larger part of the lateral loads. When the frame was at the verge of collapse, there was a total of 12,700 lbs. tension and 12,700 lbs. compression in the lateral support struts; at the same time the single forces required at the first and second hinges were 3,600 lbs. each. Thus the lateral forces at the plastic hinges made up 57 percent of the total lateral force.

To obtain a dimensionless plot of the relationship between experimental frame moments and lateral support forces, the experimental moment at the section supported was divided by the theoretical yield moment, and the lateral support force was expressed as a percentage of the axial force that would be required to cause yielding of the section if used as a very short column.

Such dimensionless plots for the lateral forces at the two plastic hinges in Frame 3 are shown in Figure 24. The curve for lateral support strut #2, located at the inside corner of the lee knee, shows lateral force of only 0.15 percent of the axial yield load at ultimate load, whereas the support force at the windward vertical load point (plastic hinge #2) was about

0.3 percent of the base value. The maximum value of any lateral support force measured during Test 3 was less than 1.0 percent of the axial yield load of the beam section.

In order that the distributions of the forces in the various lateral support struts might be seen for two critical load conditions, the isometric views of Frame 3 are given in Figure 25. The lateral forces are represented by the vectors which show the sense and the magnitude of the force. In addition, the magnitude of the force in kips is shown directly adjacent to the vector. The forces induced in the lateral bracing system by Frame 3 at ultimate load ( $P = 29.7$  kips) is shown in part "a" of Figure 25, while the condition at impending failure by lateral buckling of the lee column is shown in part "b".

Several facts illustrated by Figures 24 and 25 should be pointed out. The maximum values of the lateral forces occurred at the plastic hinges. The larger lateral forces occur at the compression flange of the beam. The presence of the lateral buckle in the top flange in the middle third of the beam is evident from the large values of lateral load in the two lateral support struts to the right of the windward vertical load point. Virtually no force was required to constrain the windward knee which was never subjected to a moment as large as the yield moment for the beam section. The forces at the top and bottom of the beam at any one section were always of opposite sense indicating that a twisting tendency always existed when the plastic condition had been reached. This tendency suggests that lateral bracing should be provided to both the compression and tension flanges of the beams.

(c) Frame 4

The behavior of Frame 4 with respect to buckling was very similar to that of Frame 3 discussed above. All instability was confined to regions which had yielded.

The first observed case of instability in Frame 4 occurred in the middle third of the beam just after the ultimate load in Phase I had been reached. The buckle of the compression flange here took the form of an "S" shape curve. The node points of the waves exactly coincided with lateral support points 4, 7, and 9. (See Figure 1(b)) These support points are 2 ft. apart. The lateral buckling of the beam may be seen in Figure 26. This photograph was taken looking down on the middle third of the beam of Frame 4. Even though this buckle developed immediately following the ultimate load in Phase I it did not prevent the frame from carrying increased horizontal loads in Phase II.

The second case of buckling in Frame 4, which finally brought about its collapse in Phase II, was a lateral buckle in the beam adjacent to the lee knee. A side view of this knee after the test is shown in Figure 27. The photograph in Figure 28 was taken looking up from the inside of the frame toward the lee knee and shows the lateral displacement of the compression flange of the beam.

The forces measured in the strut attached to the inside corner of the lee knee are plotted in Figure 29 versus the moment at the knee. In addition, the relationship between the angle of twist developed in the beam at the connection of beam to lee column and the knee moment is shown. The lateral



forces and angles of twist measured at ultimate loads, Phase I and II, are indicated on the graphs. The maximum of the lateral support forces in Frame 4 occurred in the strut (#15) used for plotting Figure 29. At ultimate load, Phase I, the maximum lateral support force was about 0.4 percent of the axial yield load. Despite the fact that Phase II was undertaken with a severely deformed frame the maximum lateral force measured at ultimate was only 1.3 percent of the axial yield load of the beam section.

The distribution of forces in the lateral support system for Frame 4 are shown in Figure 30. The ultimate load conditions for Phase I and Phase II are shown in Parts a and b, respectively. In general the lateral forces measured in Frame 4 were larger than those measured for Frame 3.

## V. S U M M A R Y

The apparatus and procedures used in testing two full-sized all-welded portal frames have been described very briefly so that the test results could be interpreted. The details of the frame and test apparatus are shown in Figures 1 and 2. The test set-up as used was satisfactory in all respects. The loading system was especially simple and allowed the testing of the frames to continue at a slow rate well after ultimate load so that much additional information was obtained.

The results of elastic and simple plastic analysis of the frames are given so that their behavior during test could be evaluated.

In this report, the major emphasis has been on the results of the tests. The following statements sum up the results.

1. The elastic behavior of the frames was for all practical purposes identical to the theoretically predicted behavior when the increased flexibility of the knees was taken into account. Methods are available by which such elastic analysis of the knee may be made (see Ref. 2).
2. The analysis of data showed that the component parts of the frame behaved in a manner that was similar to separate isolated tests of connections, beams, and columns.

3. The ultimate loads by test were 99, 97, and 95 percent, respectively, of the ultimate loads predicted by simple plastic theory for Frame 3, Frame 4(I) and Frame 4(II). (Figure 16)
4. The frames were able to carry loads very near the predicted ultimate load through deflections twice as great as those which existed when the maximum experimental load was first reached. (Figures 9 and 10)
5. The frames showed the ability to absorb relatively large amounts of energy. Frame 3 finally absorbed about 9 times as much energy as it had when the theoretical elastic limit had been reached and about 3 times as much as when the ultimate load had been reached. (Figure 9)
6. The knees used in the frames were capable of carrying more than the plastic moment for the beam section without showing any signs of failure. These high moments were carried even though the rotation of the knee finally became in one case about 5 times as great as the rotation at yield moment and 2.7 times as great as the rotation when the plastic moment of the beam section was first reached. (Figure 19)
7. The 12WF36 section used in the frames showed an ability to withstand large rotations at moments which were close to the theoretical plastic moment. The beam underwent unit rotations in the order of 16 times the theoretical unit rotation at the predicted yield moment (Figure 21). This rotation took place without flange or web crippling.

8. The magnitude of the lateral support forces required to insure the good plastic action of the frame was relatively small. The largest force measured at a single support point was about 2 percent of the theoretical axial yield load of the beam section. The maximum lateral support force measured at an ultimate load condition was 1.3 percent of the axial yield load which was measured at the plastic hinge formed at the lee knee of Frame 4(II). (Figures 24 and 29)
9. The largest lateral forces measured in either frame were at the plastic hinge locations. (Figures 25 and 30)
10. The frames were subject to lateral buckling when large regions of the beam sections became plastic. The adverse effects of this buckling were minimized by the lateral support system. All signs of plastic instability occurred after the ultimate loads had been reached. (Figures 24 and 29)
11. Final failure of Frame 3 was brought about by lateral buckling of the lee column after the frame had supported virtually its ultimate load through deflections 230 percent of those when ultimate load was first reached (see Figure 9). The column had no lateral support except at its intersection with the beam and at its base. (Figure 23)

During Phase I of Test 4 no evidence of collapse by buckling was observed. This was to be expected since the frame had not shown positive proof that it had

reached its true ultimate load when this phase of the test was discontinued.

Frame 4 finally failed in Phase II of the test when the beam adjacent to the lee knee buckled laterally. This buckling occurred when the beam center deflection was 2.6 times as large as it was at the ultimate load-Phase I. (Figure 10)

12. The 12WF36 shape was intentionally chosen to minimize the effect of local flange buckling. One small wave of flange buckling was detected in each frame soon after the ultimate load had been reached, but neither developed to any degree.

In general, the results furnish encouraging evidence of the applicability of plastic analysis in structural design. At the same time they confirm the need for adequate lateral support or other provisions for protection against lateral buckling. The lateral bracing furnished in these two tests was proved to be adequate.

## VI. A C K N O W L E D G E M E N T S

The tests and analysis described in this report are part of an investigation carried on as a result of a cooperative agreement between the Welding Research Council of the Engineering Foundation, the Navy Department, and the Institute of Research of Lehigh University. Funds are supplied by the American Institute of Steel Construction, American Iron and Steel Institute, Office of Naval Research, Bureau of Ships, and the Bureau of Yards and Docks. The investigation is being supervised by the Lehigh Project Subcommittee (T. R. Higgins, Chairman) of the Structural Steel Committee, Welding Research Council. The suggestions and guidance of this committee are gratefully acknowledged.

The tests reported herein were carried out through the efforts of several persons in addition to the authors. Much of the early planning was done by K. E. Knudsen, former Research Assistant Professor, J. P. Verschuren, former Research Assistant, designed parts of the test apparatus for Frame 3. In addition, the competent work of the laboratory machinists and technicians under the direction of K. R. Harpel, Foreman, helped bring the tests to successful conclusions.

REFERENCES

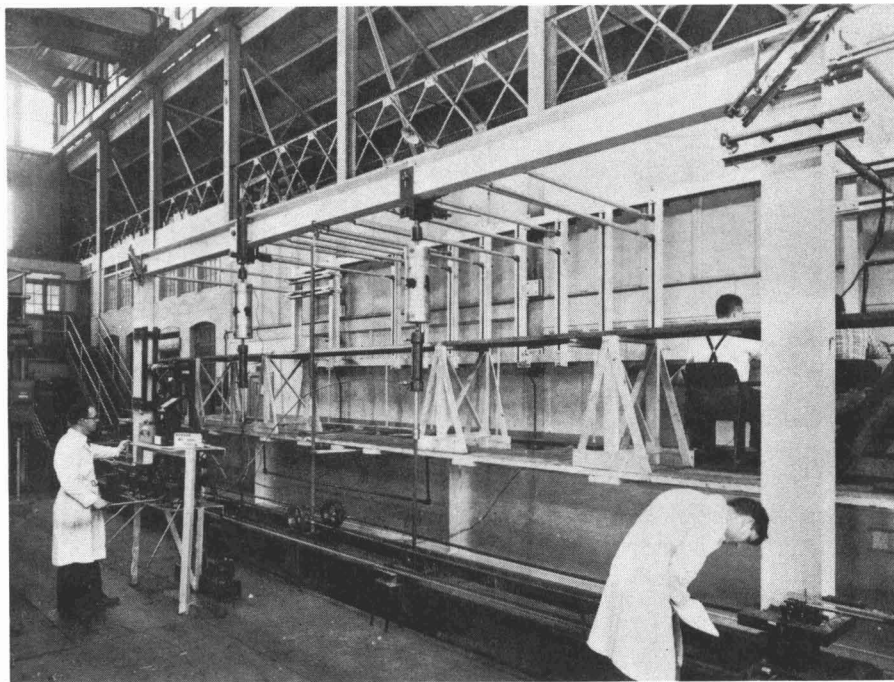
1. Ruzek, J.M., Knudsen, K.E., Johnston, E.R., and Beedle, L.S., Progress Report No. 7, "WELDED PORTAL FRAMES TESTED TO COLLAPSE", SESA Proc., Vol. XI, No. 1, 1953, Reprinted, Welding Journal, September, 1954.
2. Baker, J.F. and Roderick, J.W., "TESTS ON FULL-SCALE PORTAL FRAMES", Proc. Inst. of C.E., London, January, 1952.
3. Beedle, L.S., Topractsoglou, A.A., and Johnston, B.G., Progress Report No. 4 "CONNECTIONS FOR WELDED CONTINUOUS PORTAL FRAMES",  
Part I - "TEST RESULTS AND REQUIREMENTS FOR CONNECTIONS",  
Welding Journal, July, 1951, p. 359s.  
Part II - "THEORETICAL ANALYSIS OF STRAIGHT KNEES",  
Welding Journal, August, 1951, p. 397s.  
Part III - "DISCUSSION OF TEST RESULTS AND CONCLUSIONS",  
Welding Journal, November, 1952, p. 543s.
4. American Institute of Steel Construction, "STEEL CONSTRUCTION MANUAL", 1947.
5. Symonds, P.S. and Neal, B.G., "RECENT PROGRESS IN PLASTIC METHODS OF STRUCTURAL ANALYSIS", Journal of the Franklin Institute, Vol. 252 No. 5 and 6.
6. Baker, J.F. and Horne, M.R., "NEW METHODS IN THE ANALYSIS AND DESIGN OF STRUCTURES IN THE PLASTIC RANGE", British Welding Journal, 1(7) p. 307, July, 1954.
7. British Constructional Steelwork Association, "THE COLLAPSE METHOD OF DESIGN", B.C.S.A. Publication No. 5, 1952.
8. Yang, C.H., Beedle, L.S., and Johnston, B.G., Progress Report No. 3, "PLASTIC DESIGN AND THE DEFORMATION OF STRUCTURES", Welding Journal, July, 1951, p. 348s.
9. Lewis, E.M., "CONSTRUCTION OF THE B.W.R.A. TESTING LABORATORY", British Welding Journal, 1(12), December, 1954.
10. Haaijer, G. and Thürlimann, B., "LOCAL BUCKLING OF WIDE-FLANGE SHAPES", Fritz Laboratory Report 205E.5., December, 1954.

## N O M E N C L A T U R E

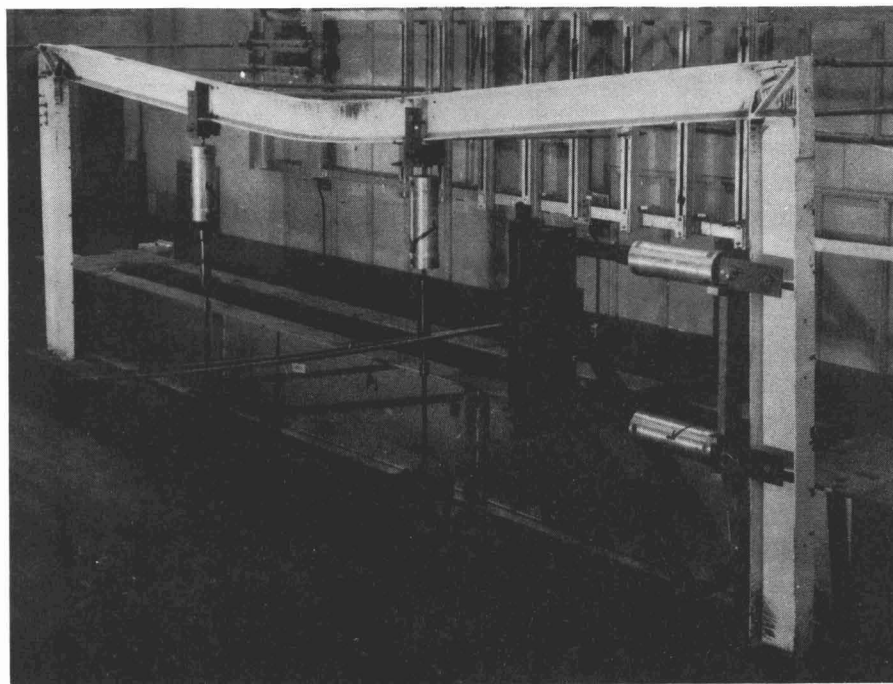
E	=	Young's modulus of elasticity
H	=	Horizontal reaction
$I_x$	=	Moment of inertia
LB	=	(in figures) Point of which lateral buckling occurred
M	=	Moment
$M_p$	=	Full plastic moment
$M_y$	=	Moment at which yield point is reached in flexure
P	=	Concentrated vertical load
$P_p$	=	Theoretical ultimate concentrated vertical load
$P_y$	=	Theoretical first yield concentrated vertical load
Q	=	Concentrated horizontal load
$Q_p$	=	Theoretical ultimate concentrated horizontal load
$Q_y$	=	Theoretical first yield concentrated horizontal load
$S_x$	=	Section modulus, $\frac{I}{c}$
UL	=	(in figures) Ultimate load
YL	=	(in figures) First observed yield line
$Z_x$	=	Plastic modulus, $Z_x = \frac{M_p}{\sigma_y}$
$\alpha$	=	Lateral angle of twist
$\delta$	=	Deflection
$\epsilon_{st}$	=	Strain at strain-hardening
$\sigma_y$	=	Yield stress level
$\phi$	=	Rotation per unit length, or average unit rotation; curvature





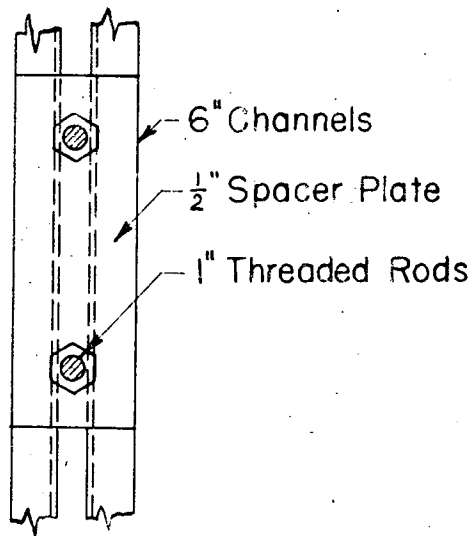
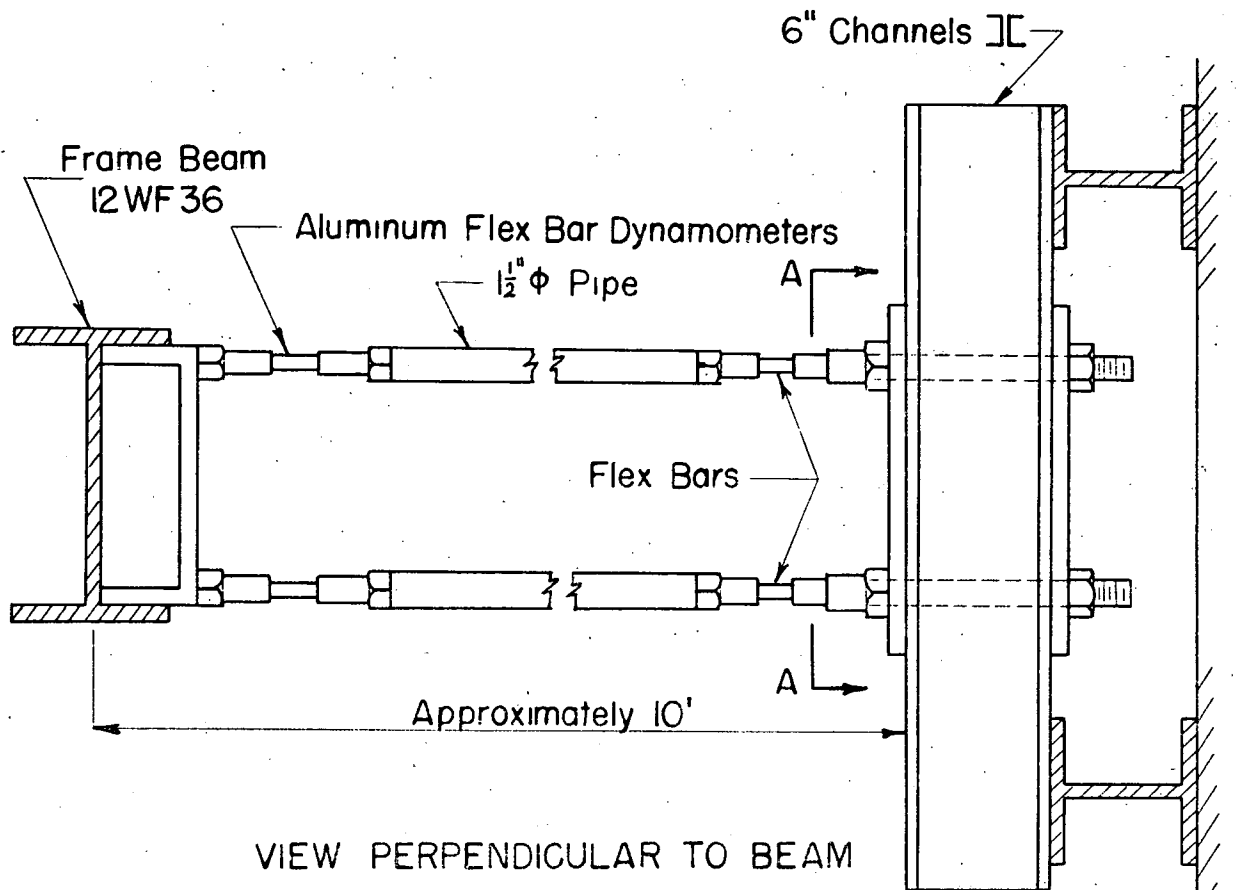


(a) Frame 3 Before Test



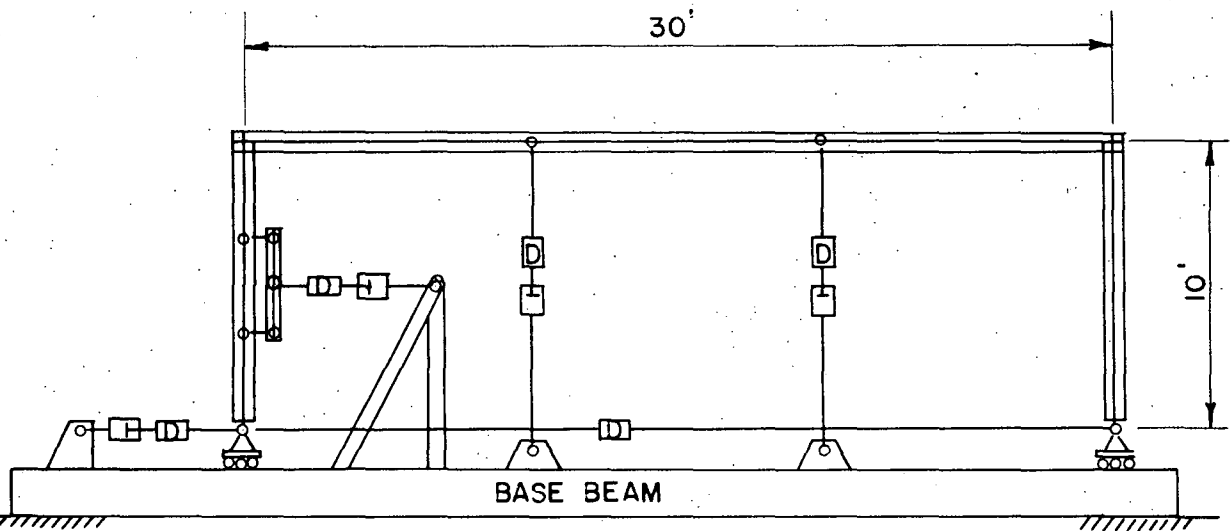
(b) Frame 4 After Test

Fig. 2 General Views of Frames


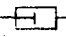


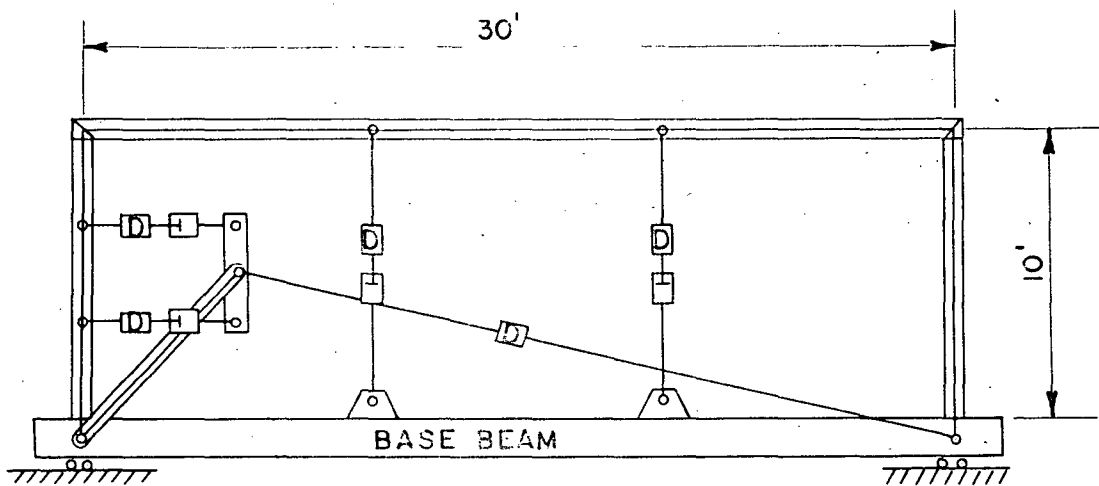
SECTION A-A

FIG. 3 LATERAL SUPPORT STRUTS



a. FRAME 3

LEGEND:  — LOAD DYNAMOMETER  
 — HYDRAULIC TENSION JACK



b. FRAME 4

FIG. 4 SCHEMATIC OF LOADING SYSTEMS

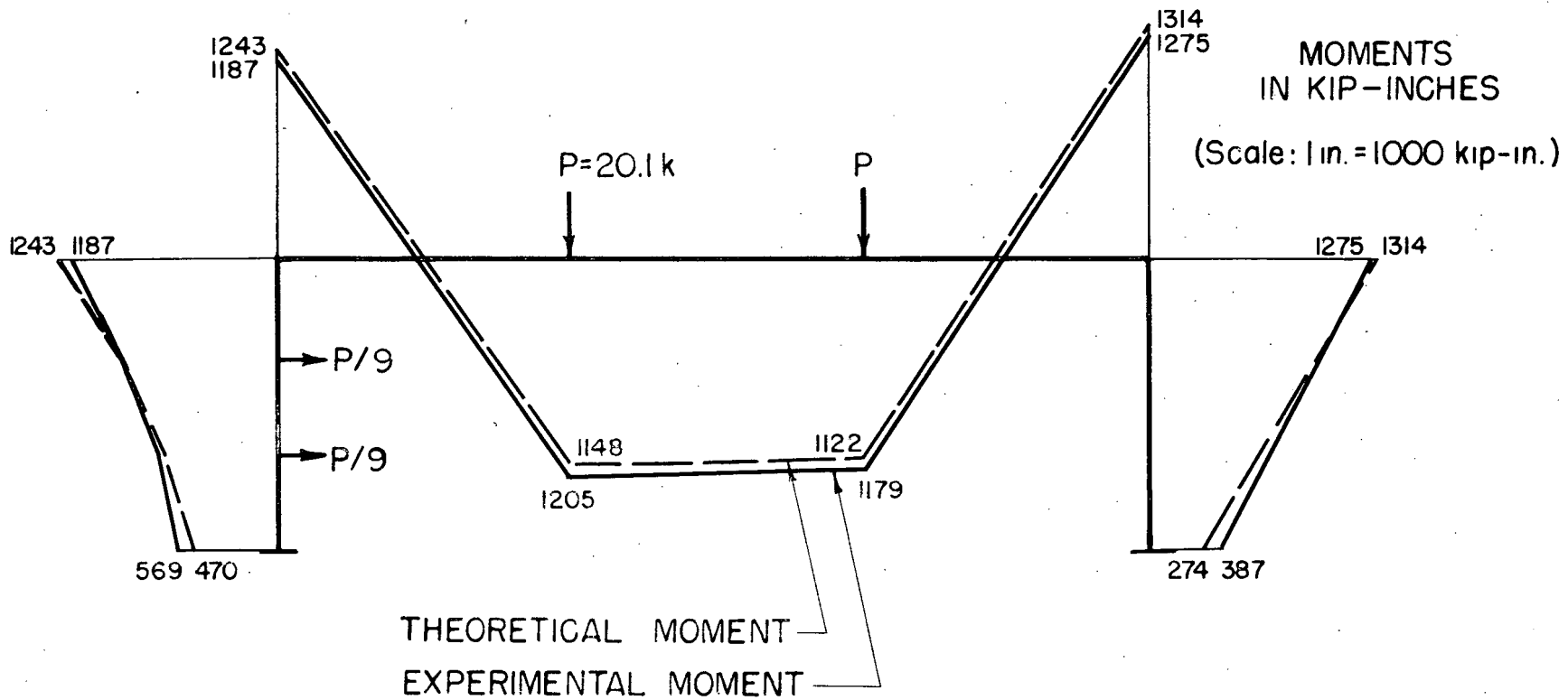


FIG. 5 COMPARISON OF THEORETICAL AND EXPERIMENTAL MOMENTS FOR FRAME 4 IN ELASTIC STATE

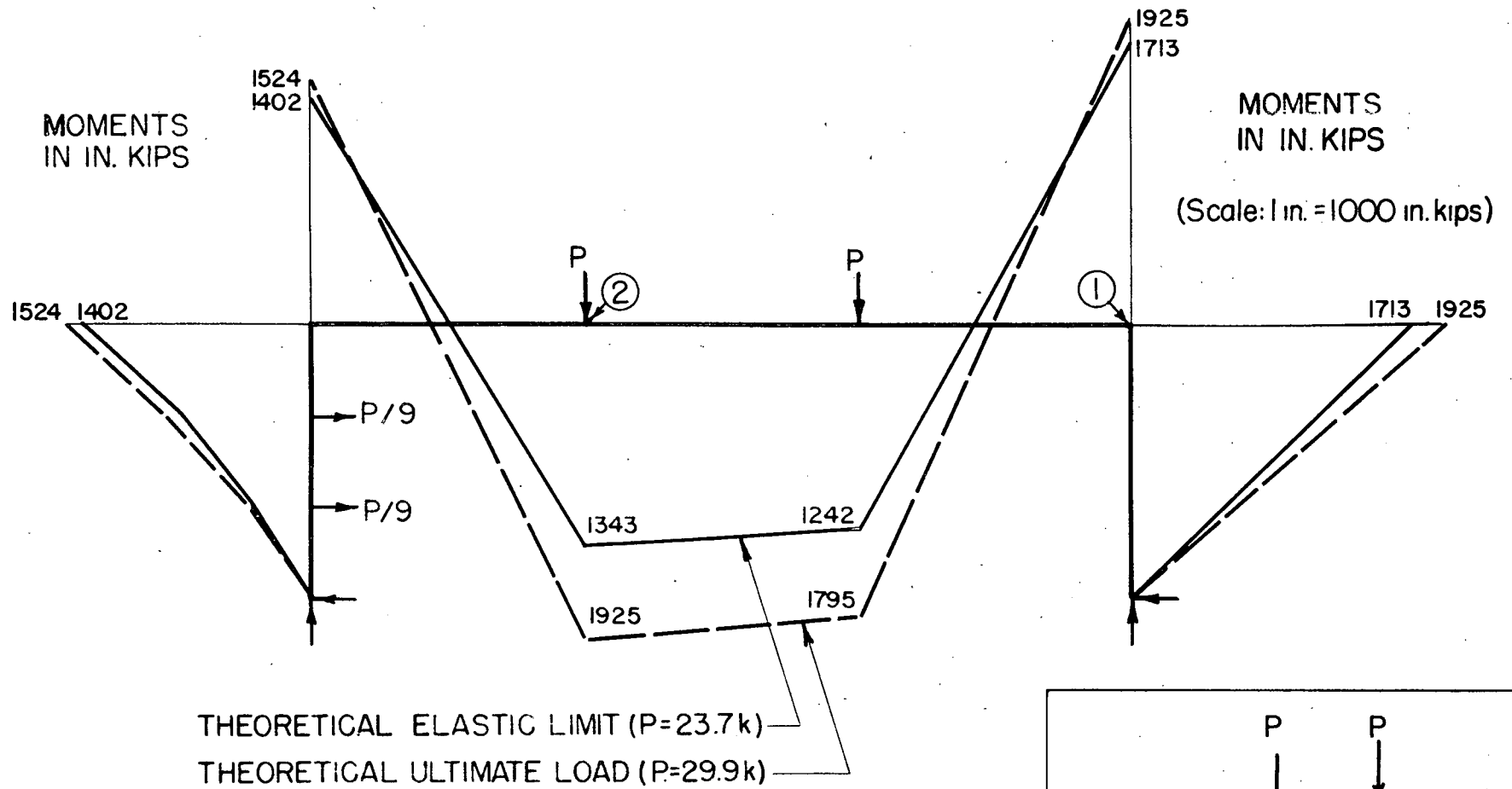
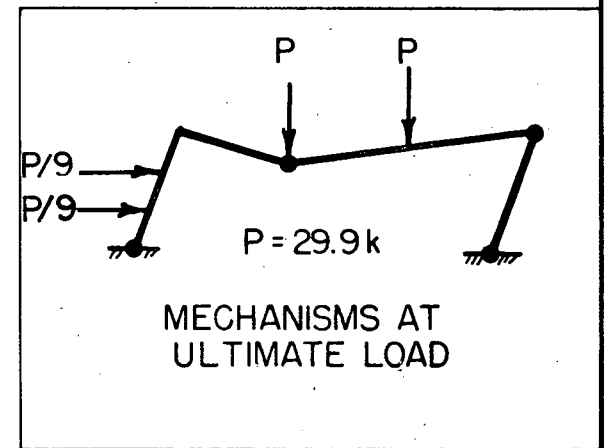


FIG.6 THEORETICAL MOMENT DIAGRAMS FOR FRAME 3





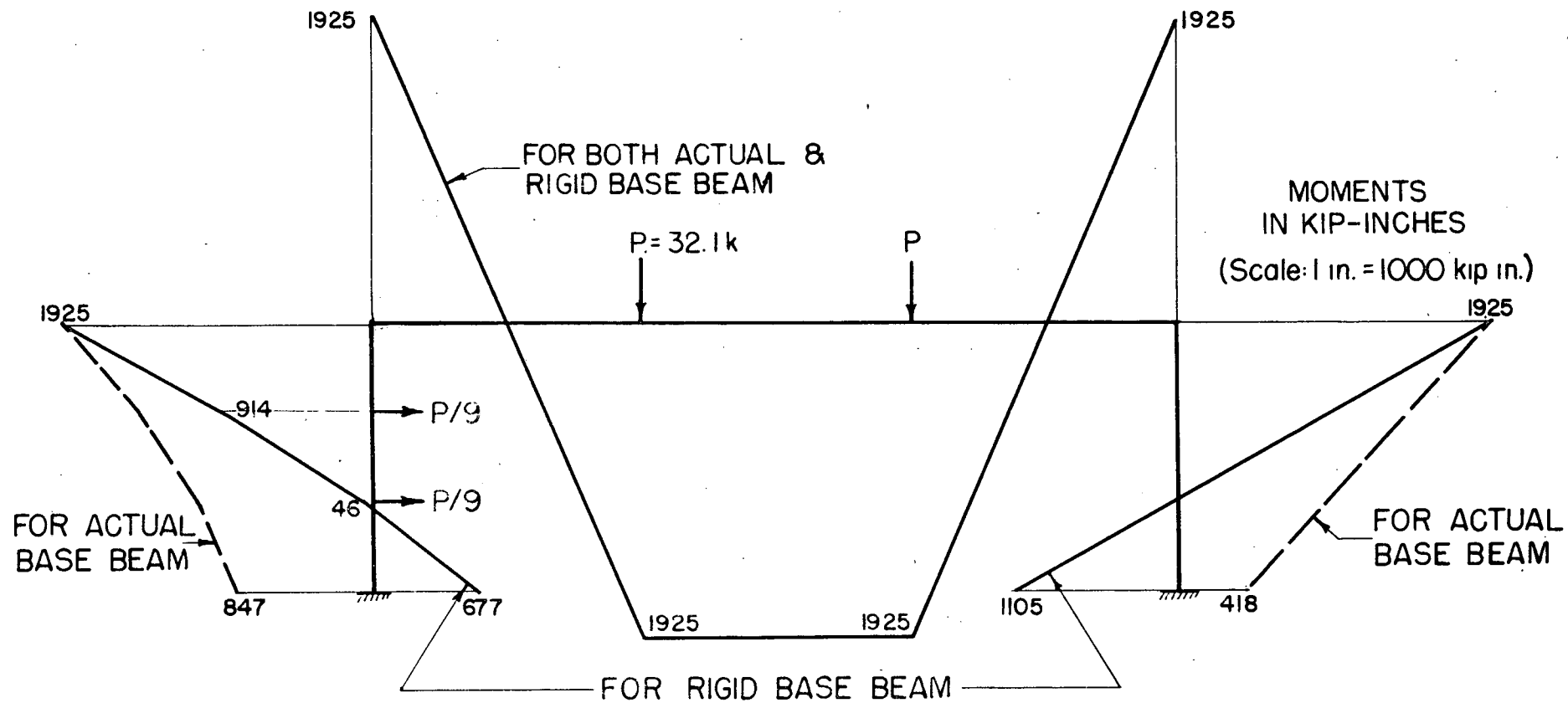


FIG. 8 BASE BEAM RIGIDITY EFFECT ON ULTIMATE LOAD MOMENTS - FRAME 4 (I)



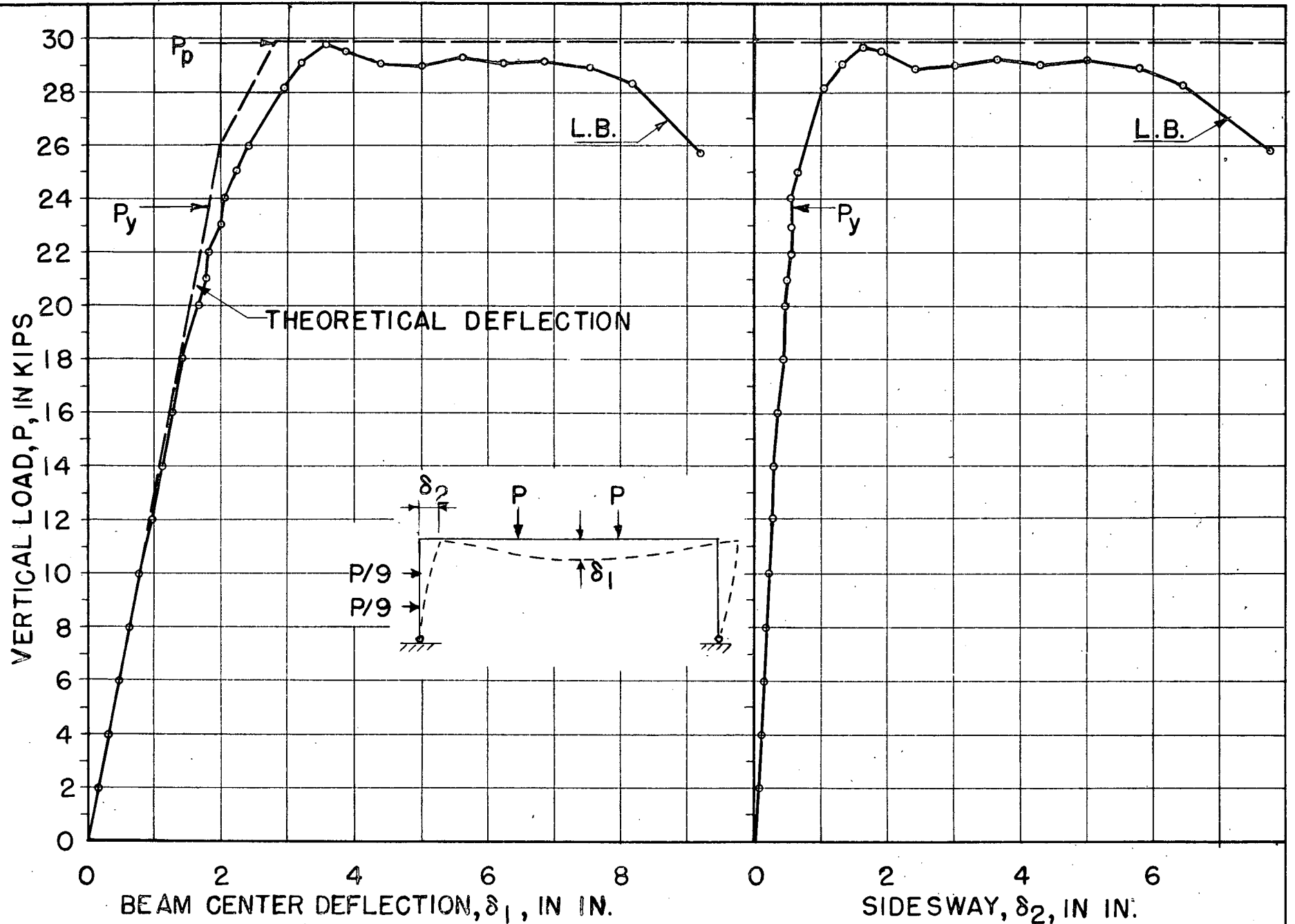


FIG. 9 LOAD-DEFLECTION CURVES-FRAME 3

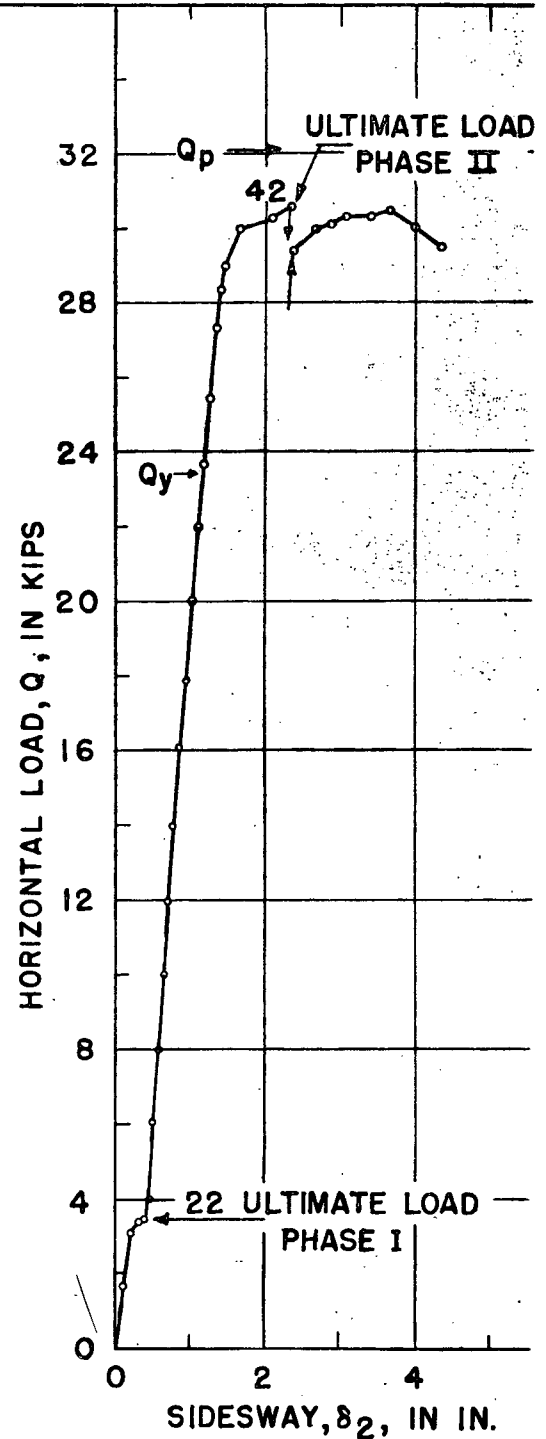
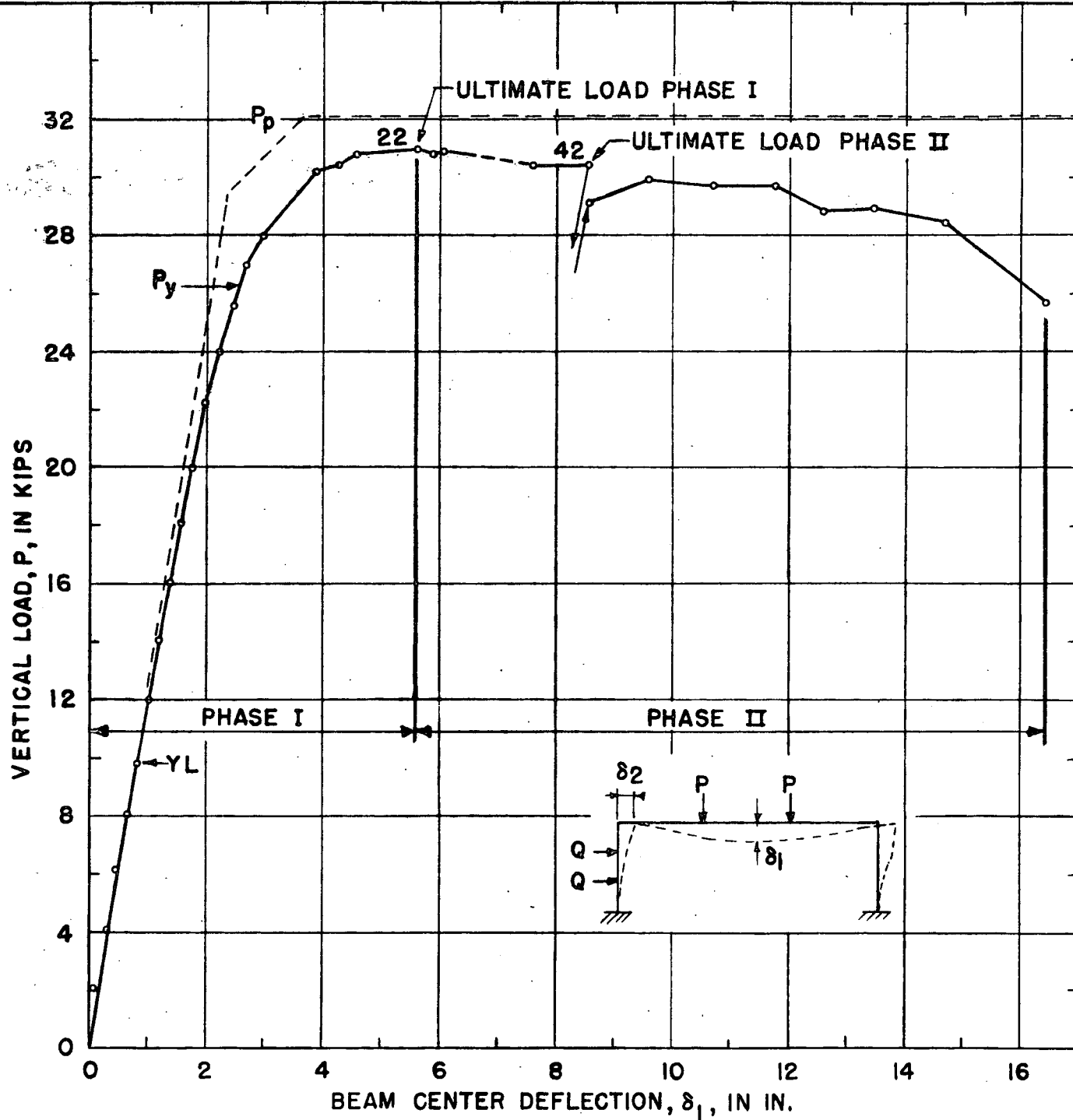
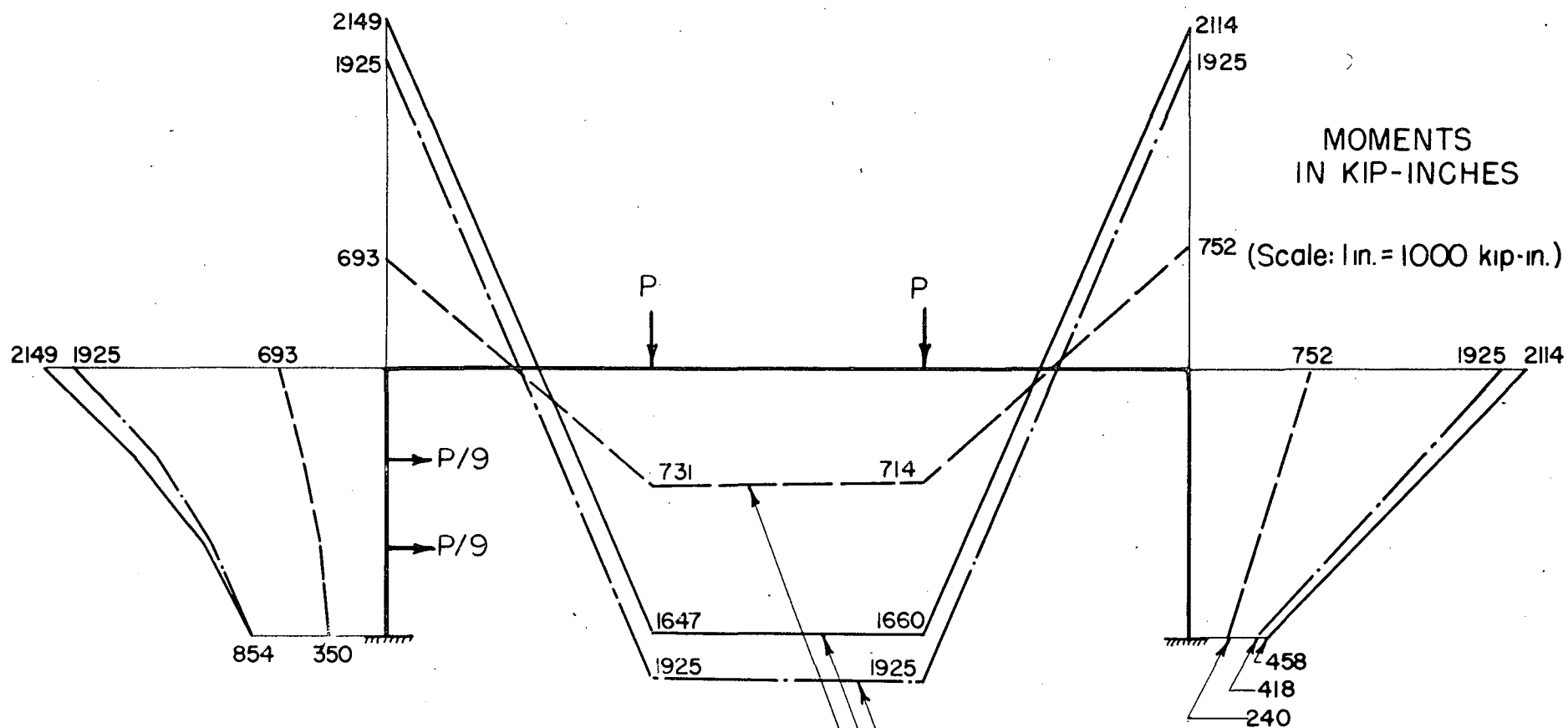


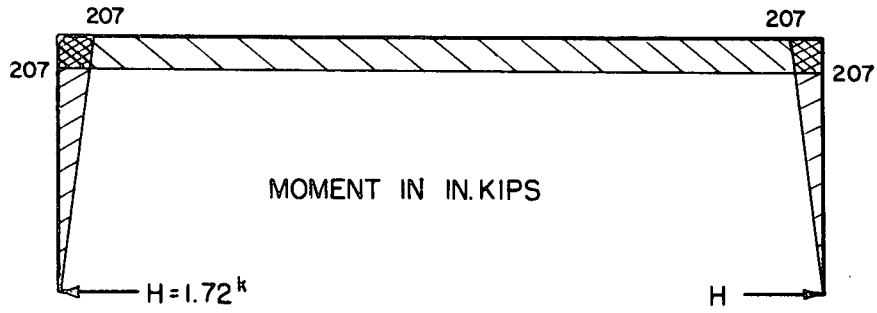
FIG.10 LOAD-DEFLECTION CURVES FOR FRAME 4



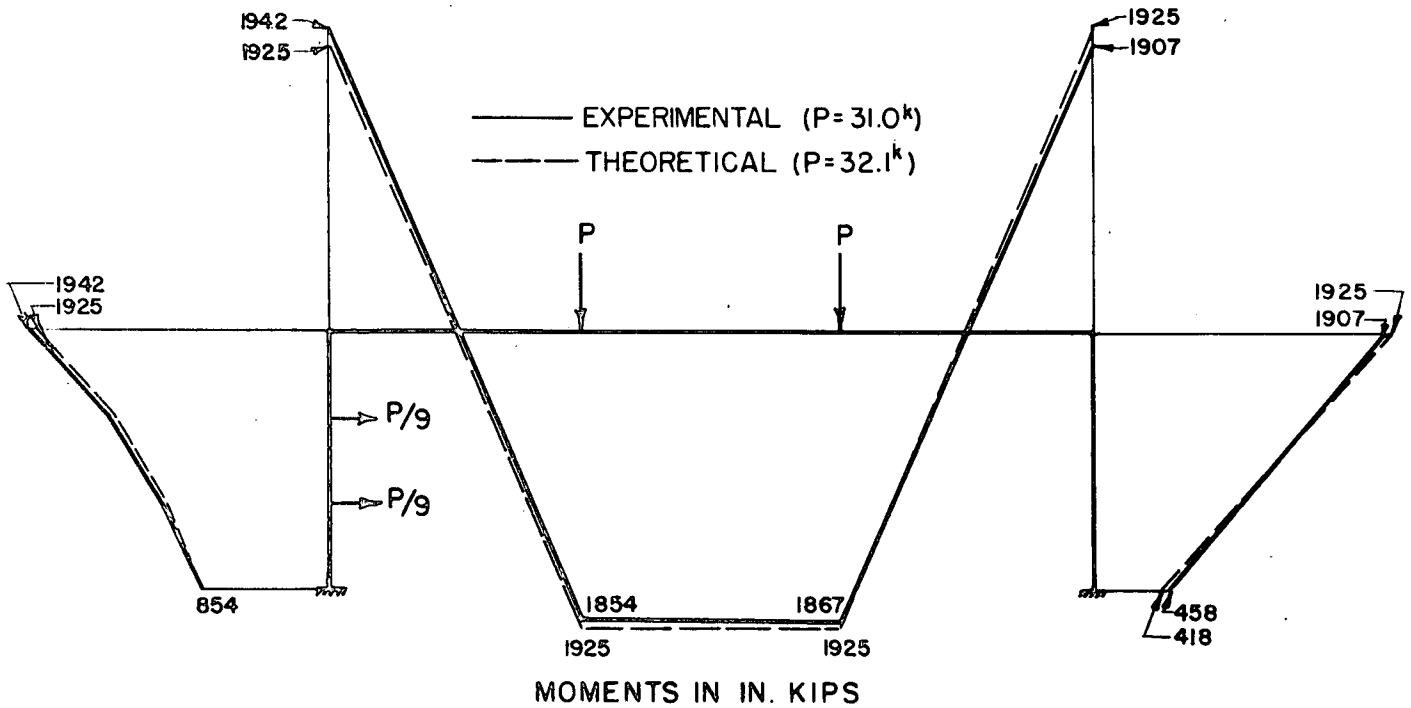


EXPERIMENTAL BENDING STRESS = 17.14 ksi (P=12.0k)  
 EXPERIMENTAL ULTIMATE LOAD (P= 31.0k)  
 THEORETICAL ULTIMATE LOAD (P= 32.1k)

FIG.12 THEORETICAL AND EXPERIMENTAL MOMENT  
 DIAGRAMS FOR FRAME 4 - PHASE I

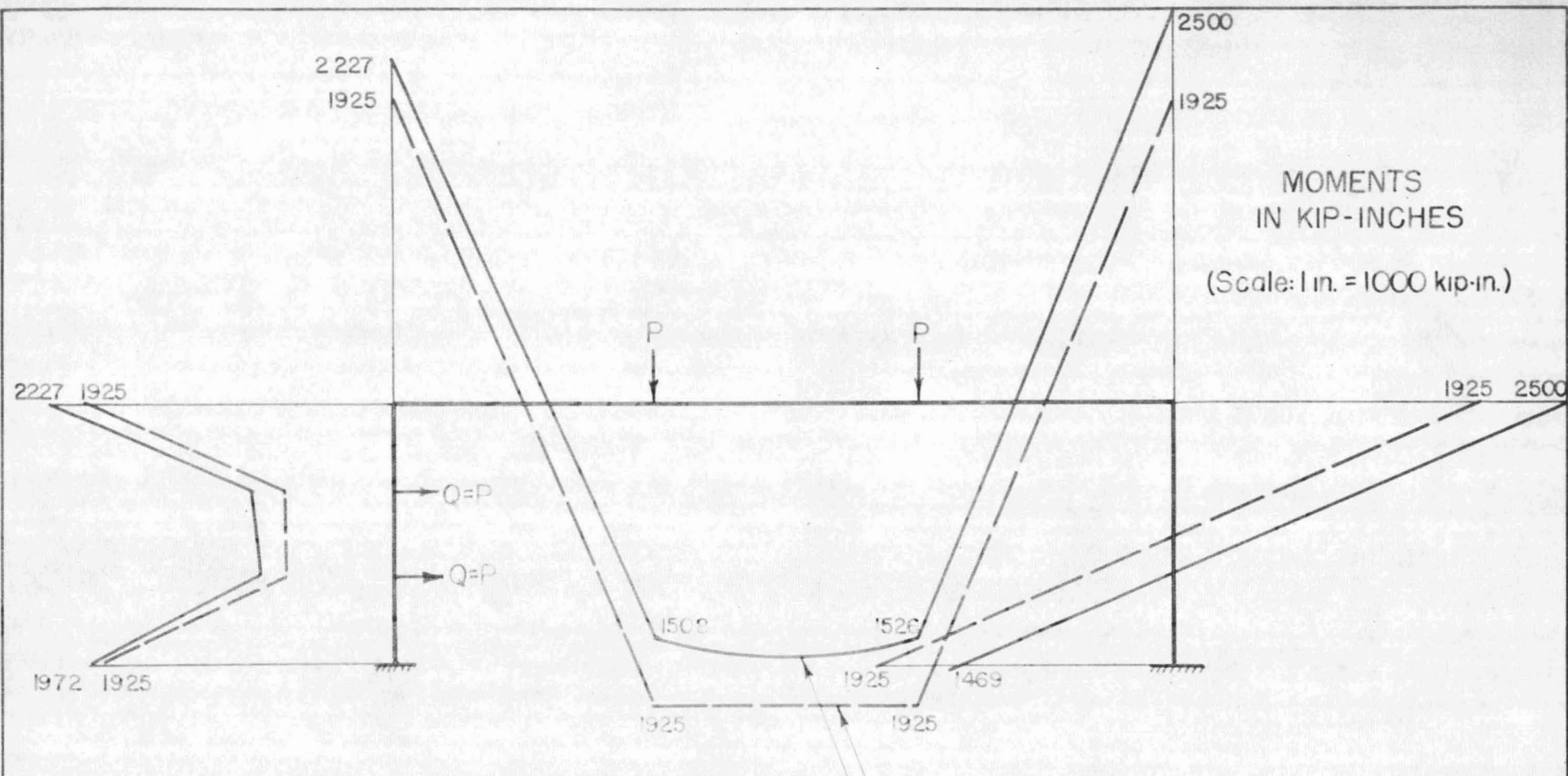


(a) "LOCKED-UP" MOMENTS CAUSED BY SPREADING OF COLUMN BASES PRIOR TO WELDING



(b) CORRECTED EXPERIMENTAL MOMENT DIAGRAM AT ULTIMATE LOAD

FIG.13 EFFECT OF "LOCKED-UP" MOMENTS IN FRAME 4-PHASE I



EXPERIMENTAL ULTIMATE LOAD (Q=30.2k)  
THEORETICAL ULTIMATE LOAD (Q=32.1k)

FIG. 14 THEORETICAL AND EXPERIMENTAL MOMENTS AT ULTIMATE LOAD, FRAME 4 - PHASE II

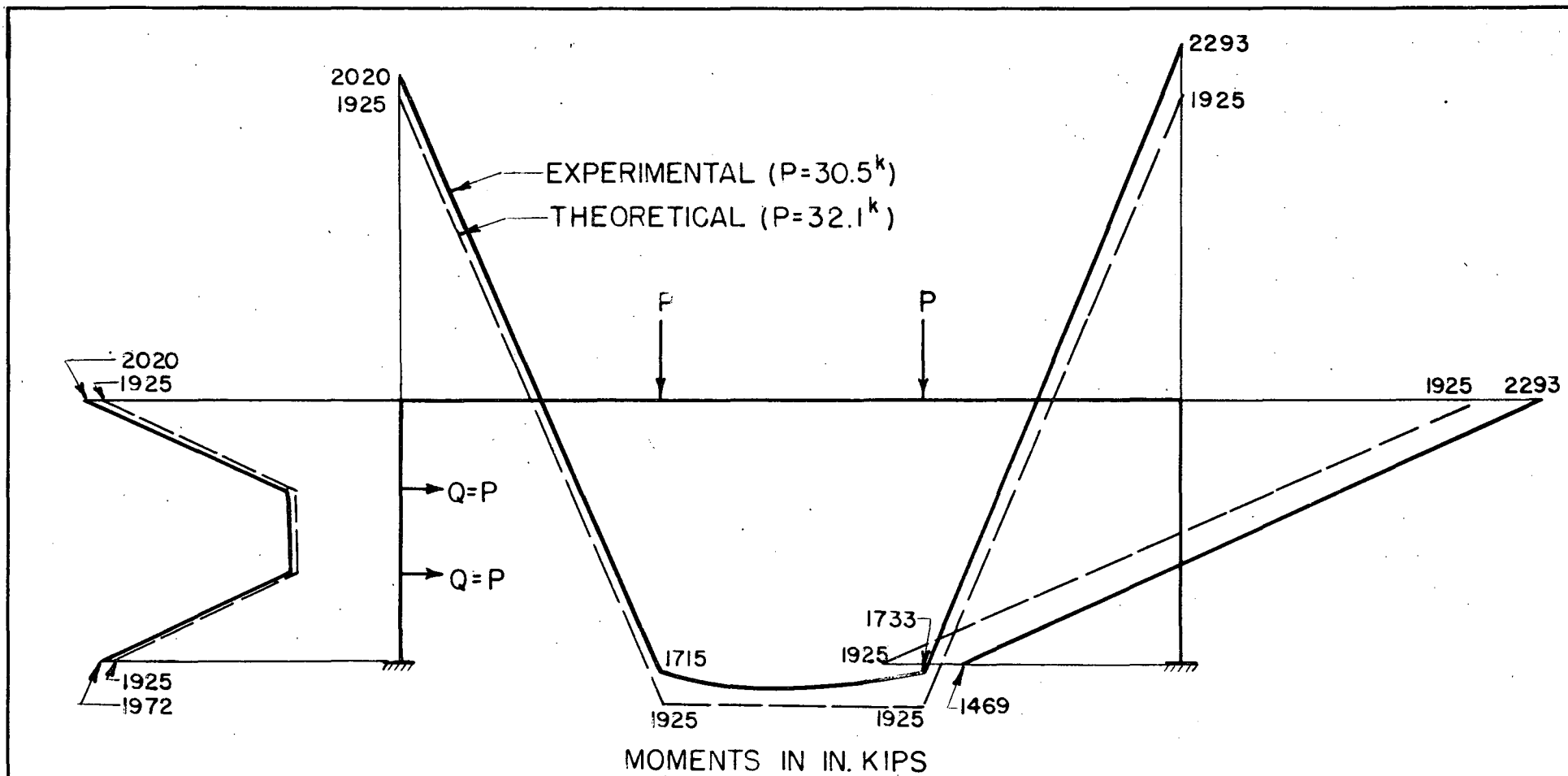


FIG.15 EXPERIMENTAL MOMENTS CORRECTED FOR "LOCKED-UP" MOMENTS FRAME 4-PHASE II

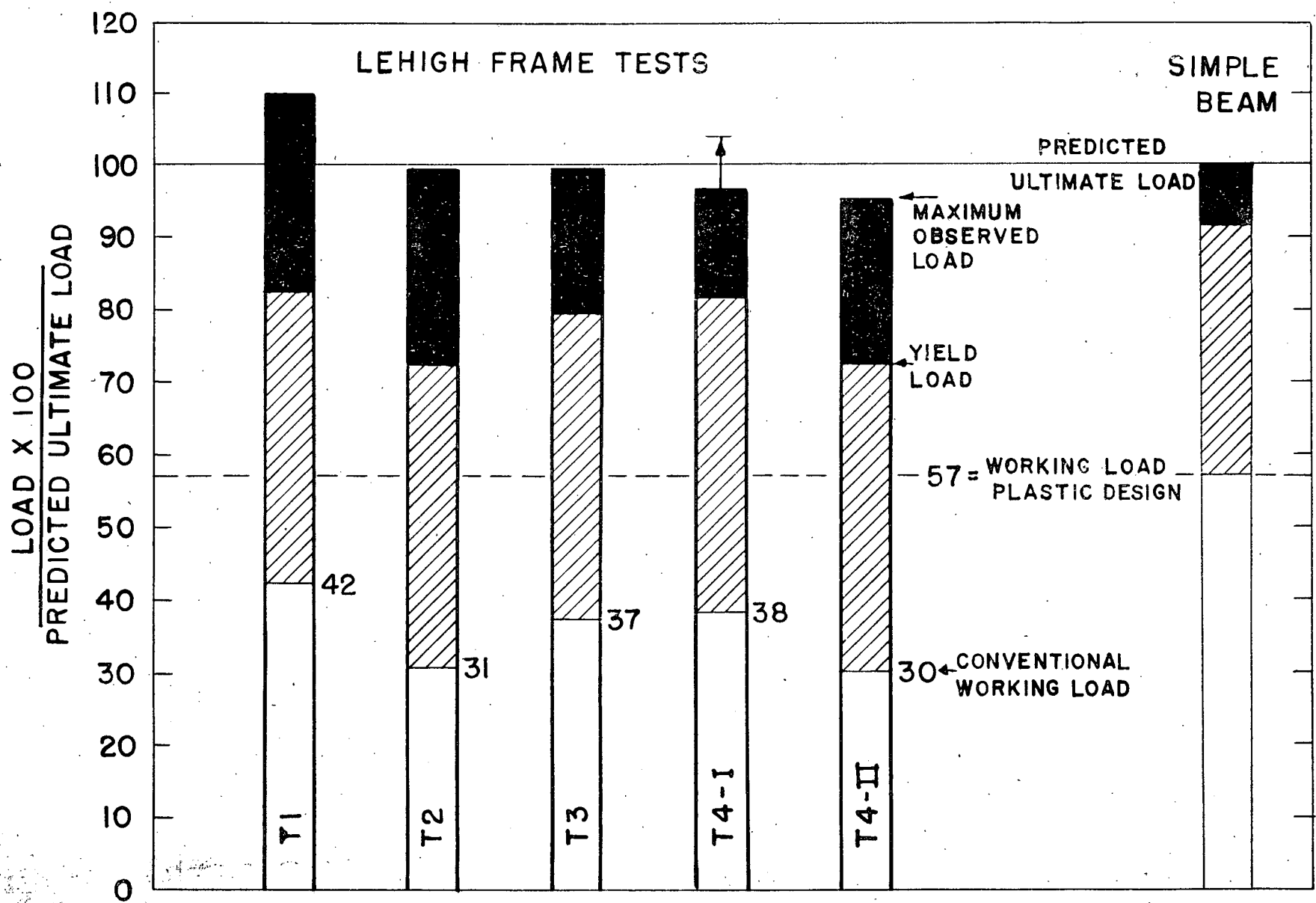
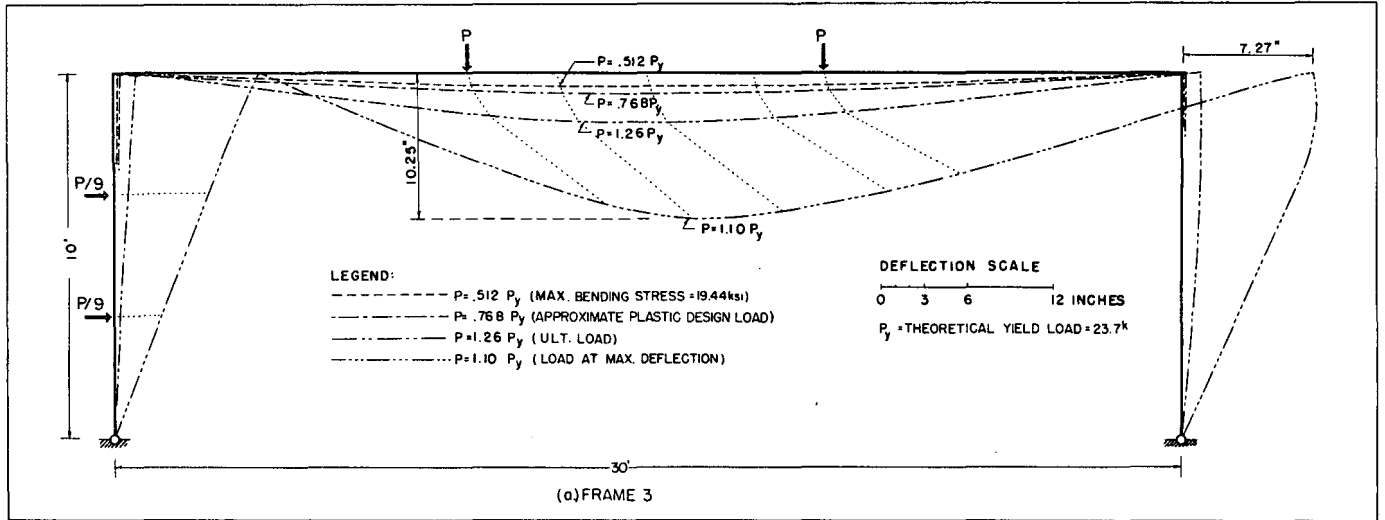


FIG. 16 BAR CHART OF FRAME STRENGTHS



2020-117



2020-118

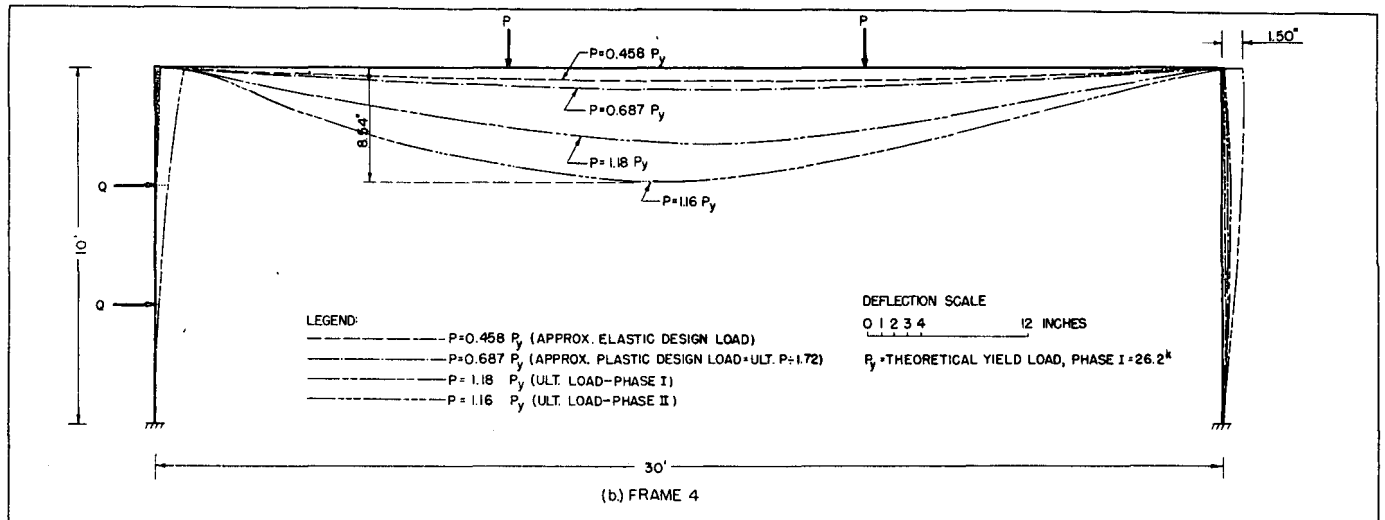
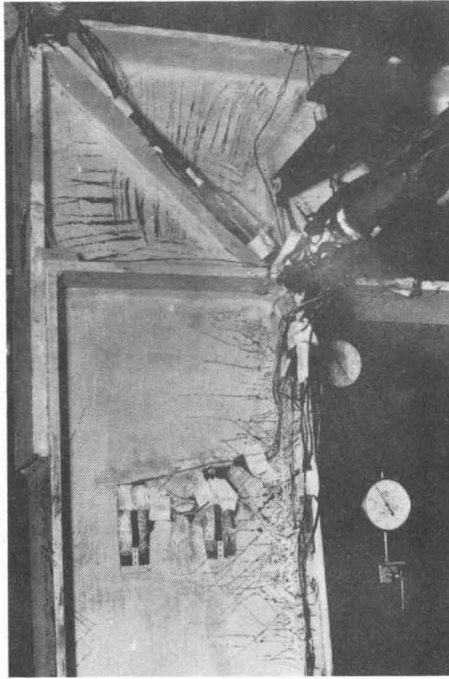
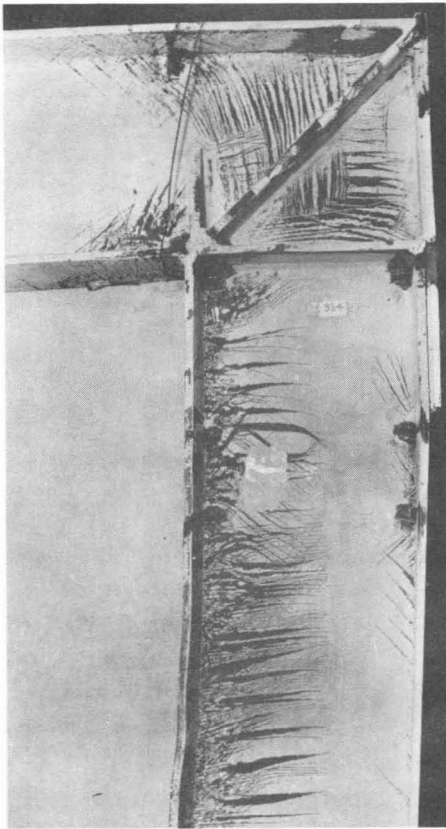


FIG. 17 DEFLECTED FRAME SHAPES



(a) At Ultimate Load



(b) After Completion of Test

Fig. 18 Lee Knee - Frame 3

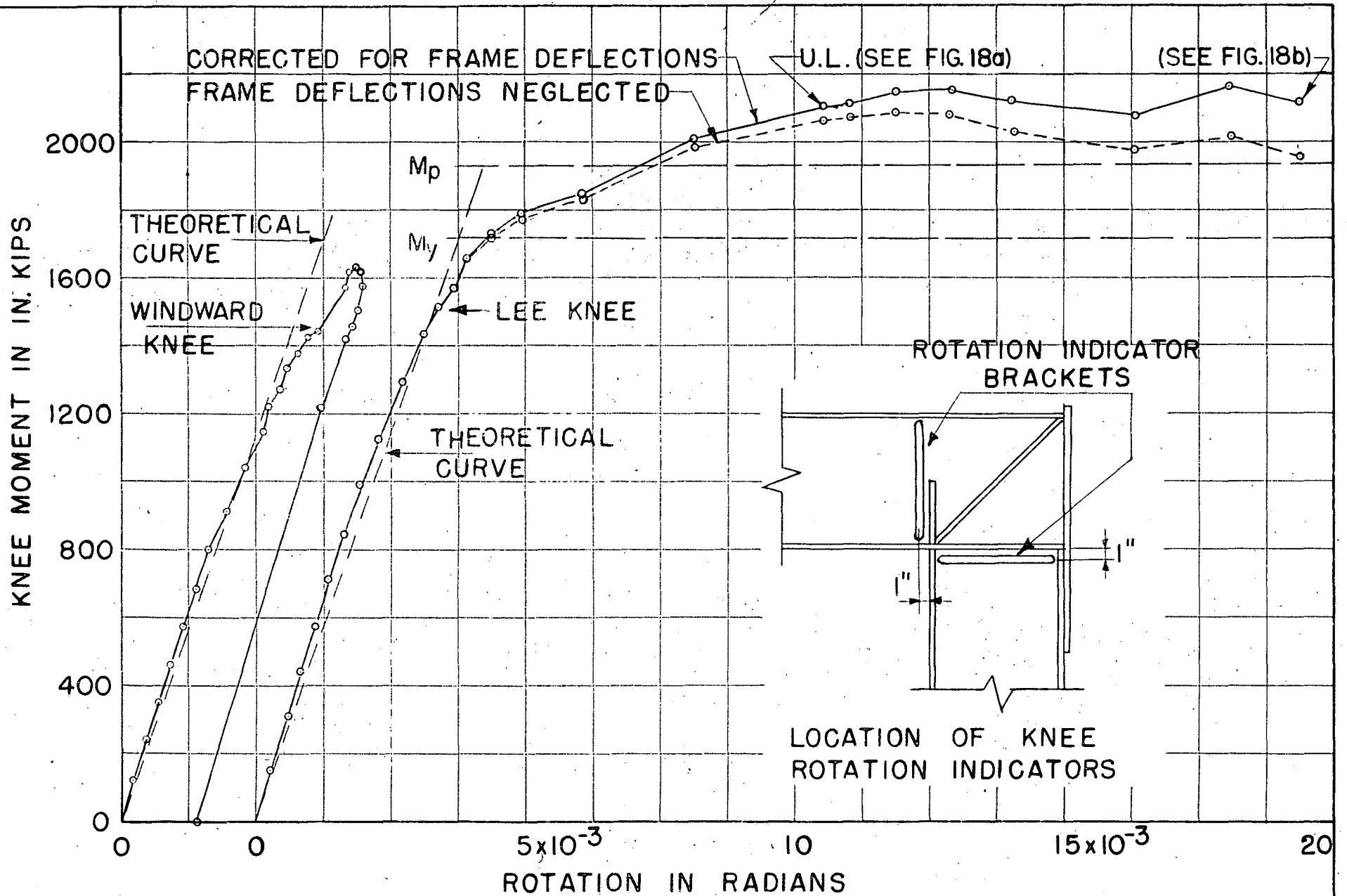


FIG. 19 MOMENT-ROTATION CURVES FOR KNEES-FRAME 3

28x10<sup>2</sup>

KNEE MOMENT IN INCH KIPS

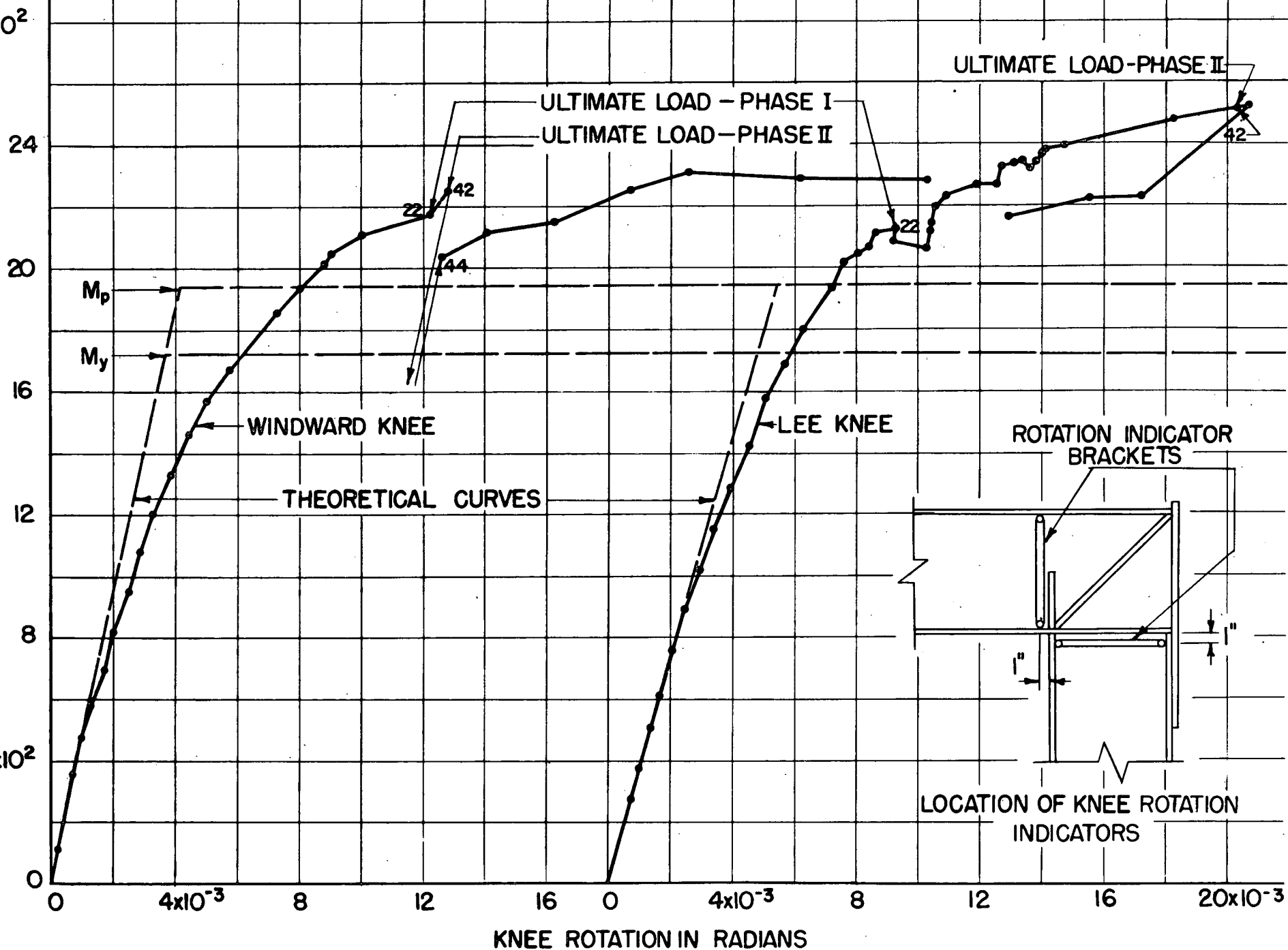


FIG. 20 MOMENT ROTATION CURVES FOR FRAME 4 KNEES

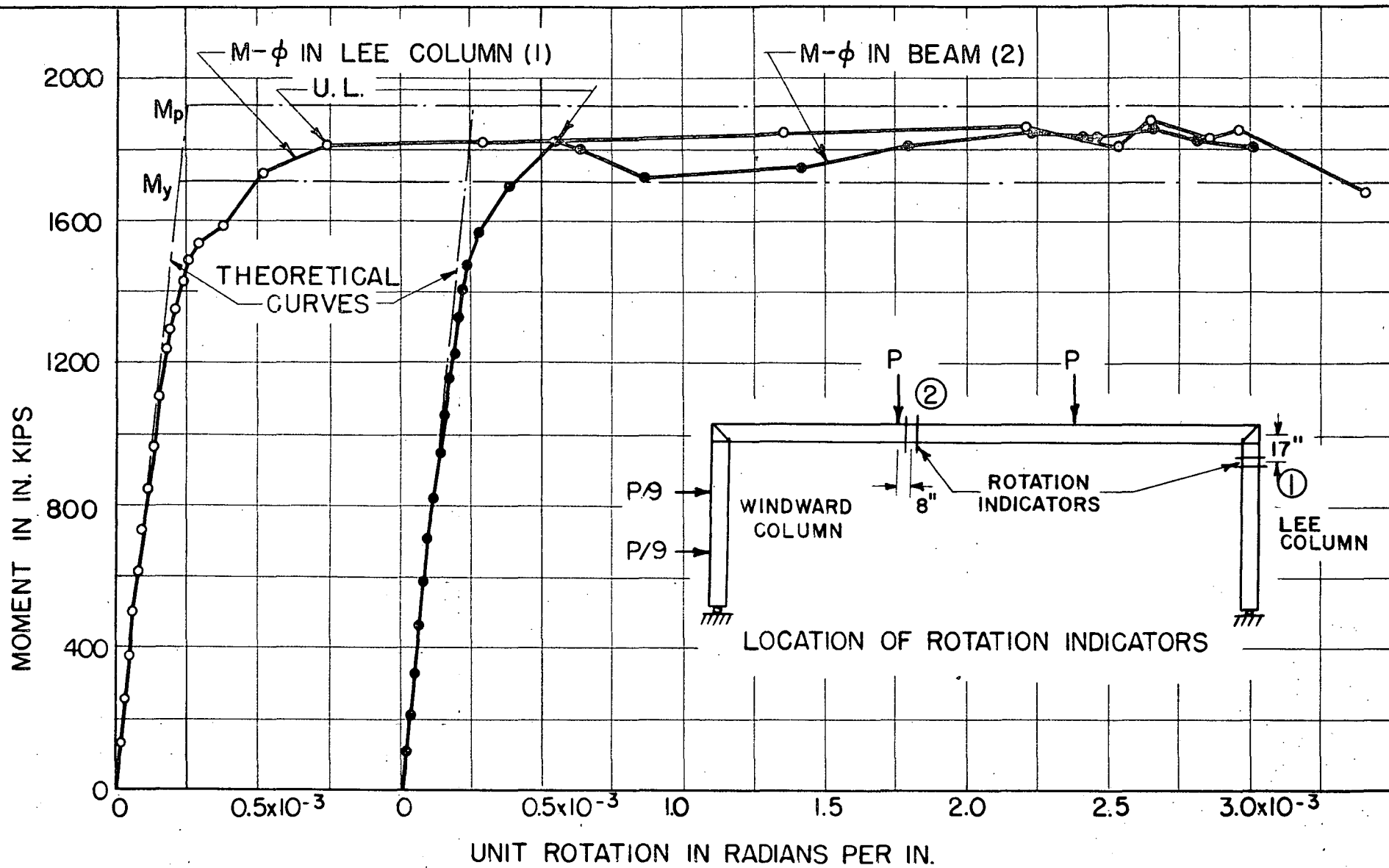


FIG.21 MOMENT-UNIT ROTATION CURVES FOR SECTIONS IN FRAME 3

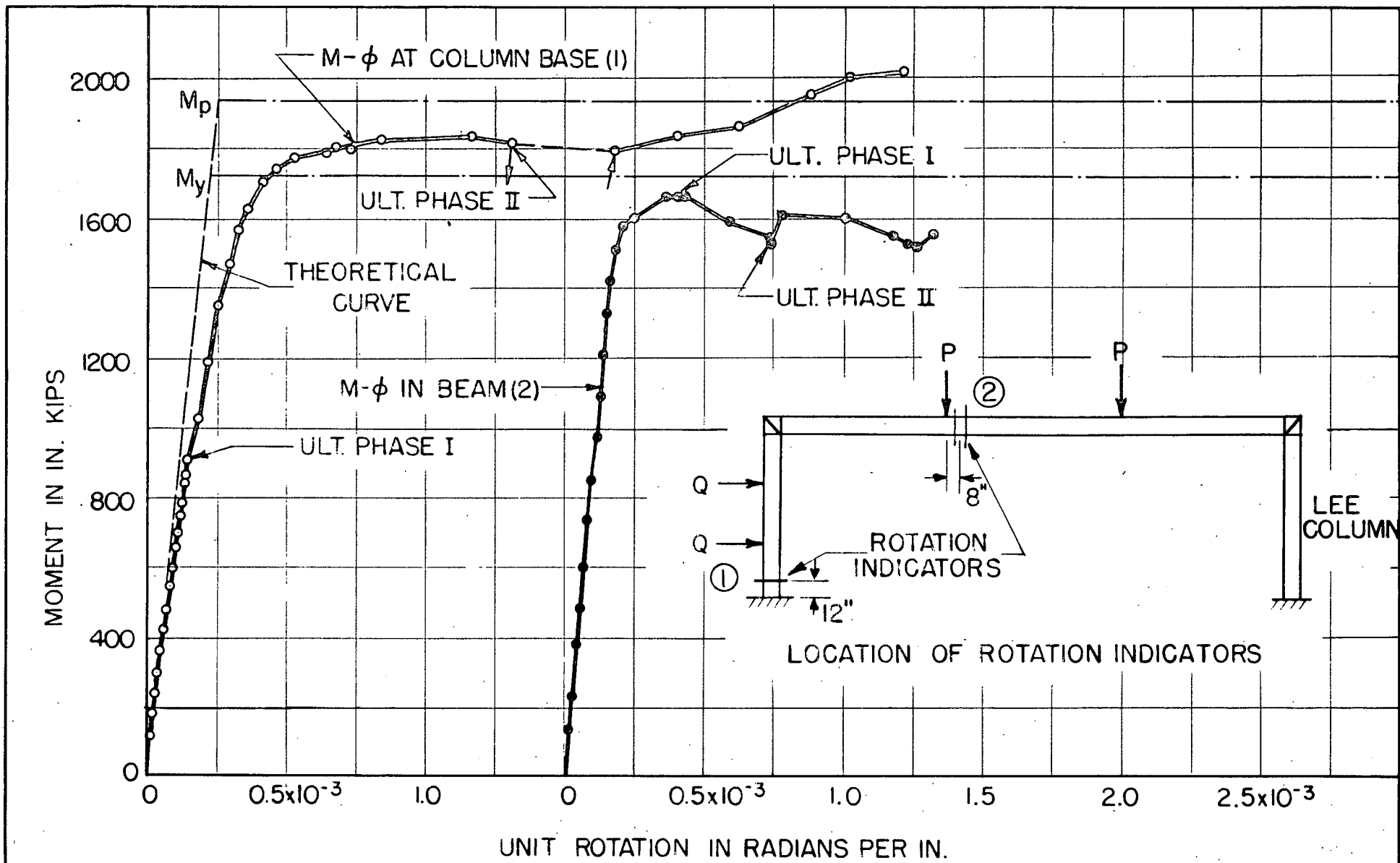


FIG.22 MOMENT-UNIT ROTATION CURVES FOR SECTIONS IN FRAME 4

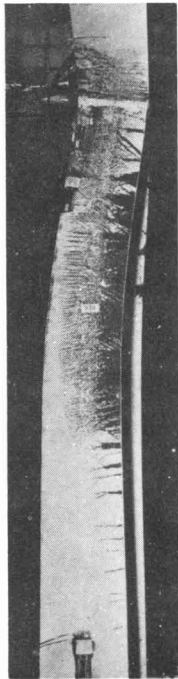


Fig. 23 Lateral Buckle  
in Lee Column - Frame 3

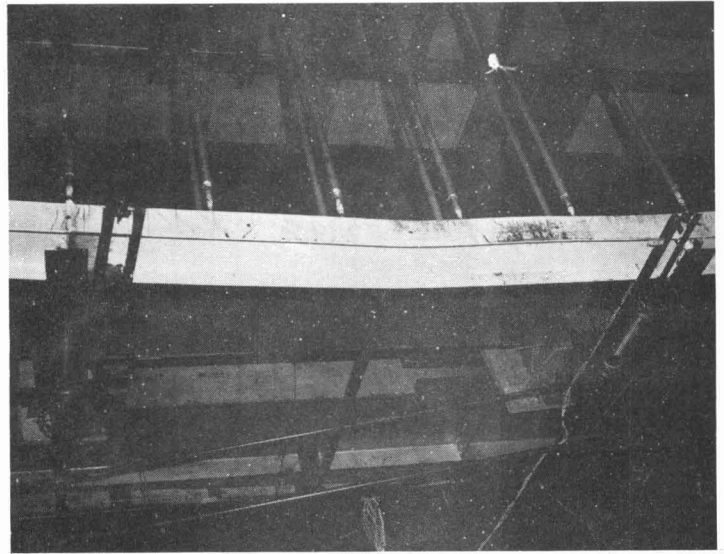


Fig. 26 Top View Showing Lateral Buckle  
in Middle Third of Beam - Frame 4

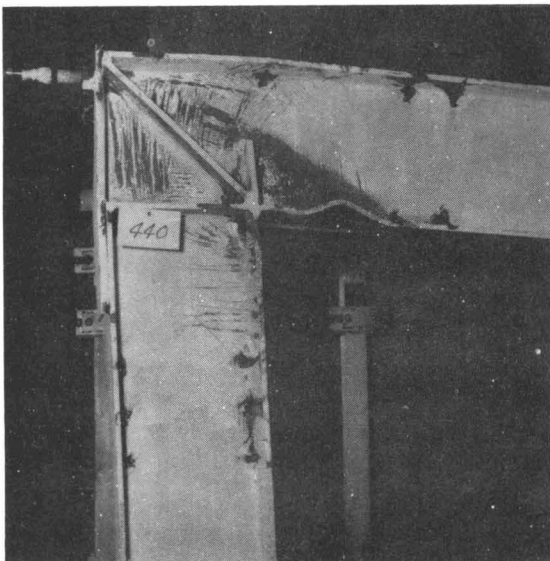


Fig. 27 Lee Knee After Test  
Frame 4

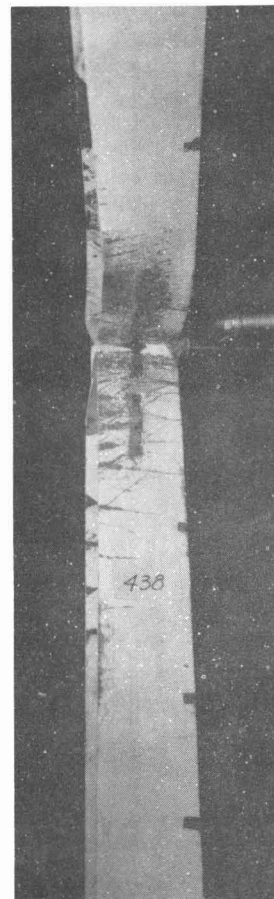


Fig. 28 View Looking Up at Lateral  
Buckle in Beam at Lee Knee  
Frame 4

23, 26, 27, 28

2050-123

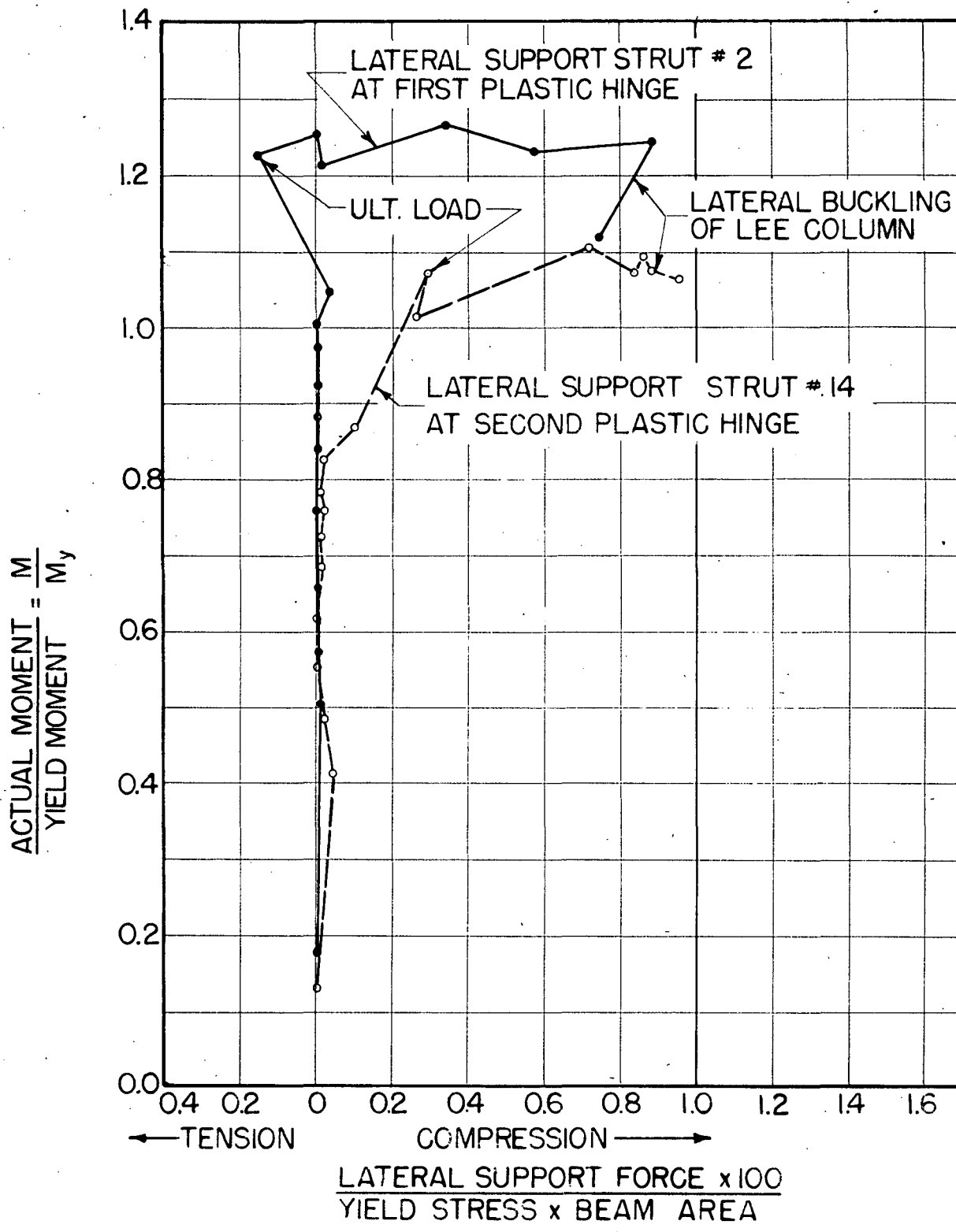
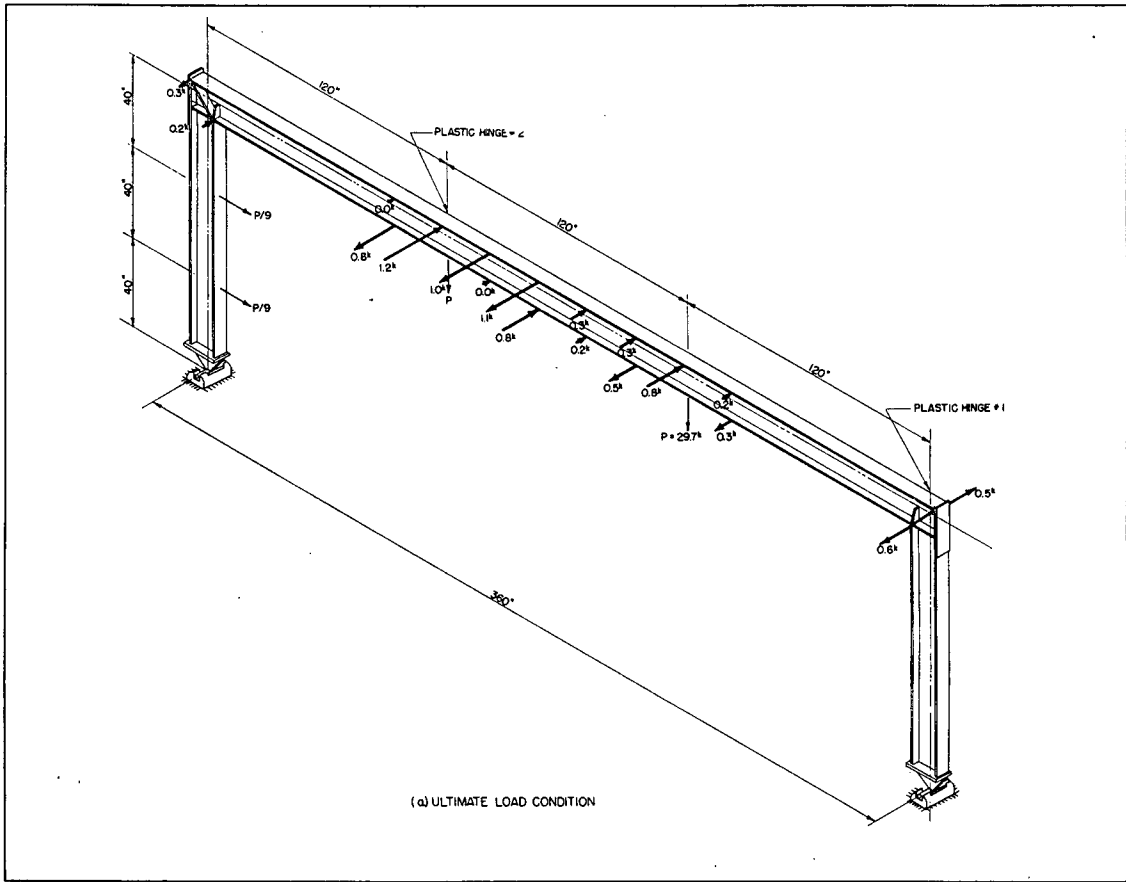


FIG. 24 LATERAL SUPPORT FORCES AT PLASTIC HINGES IN FRAME 3



2050-124



2050-125

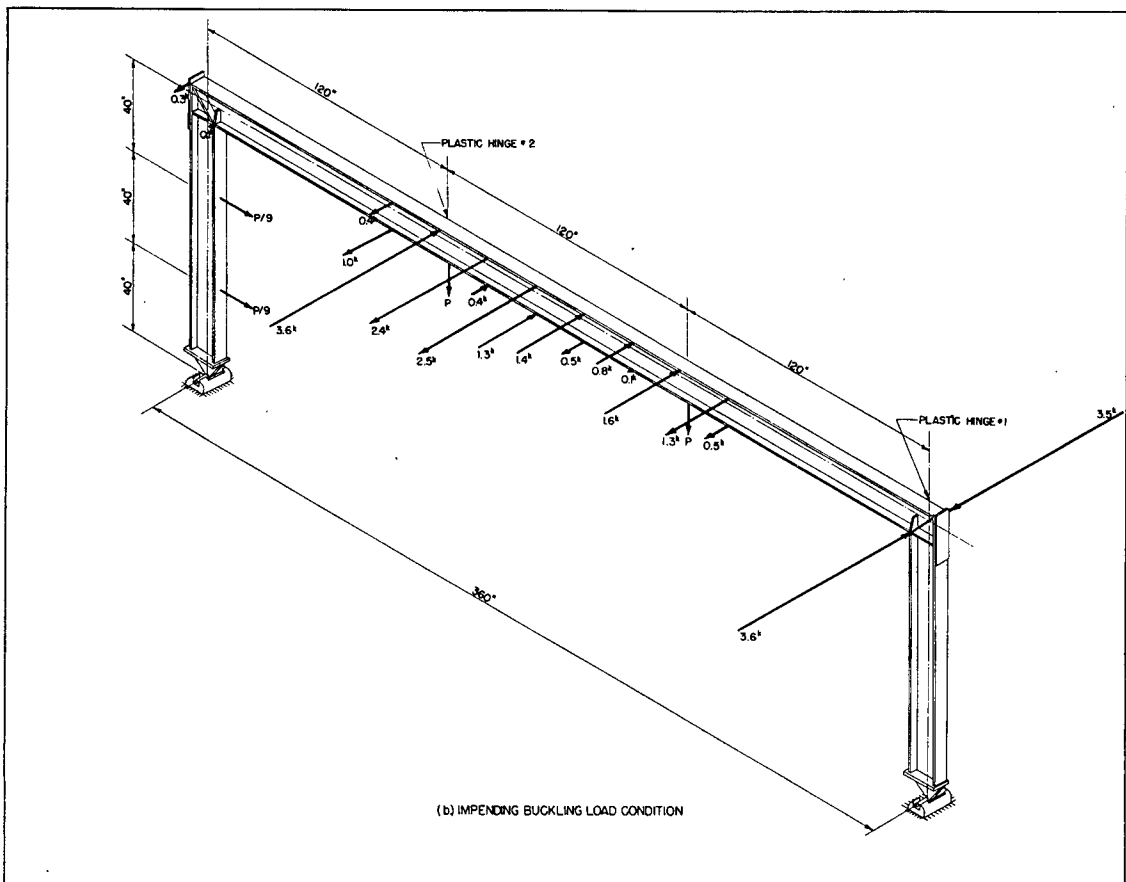
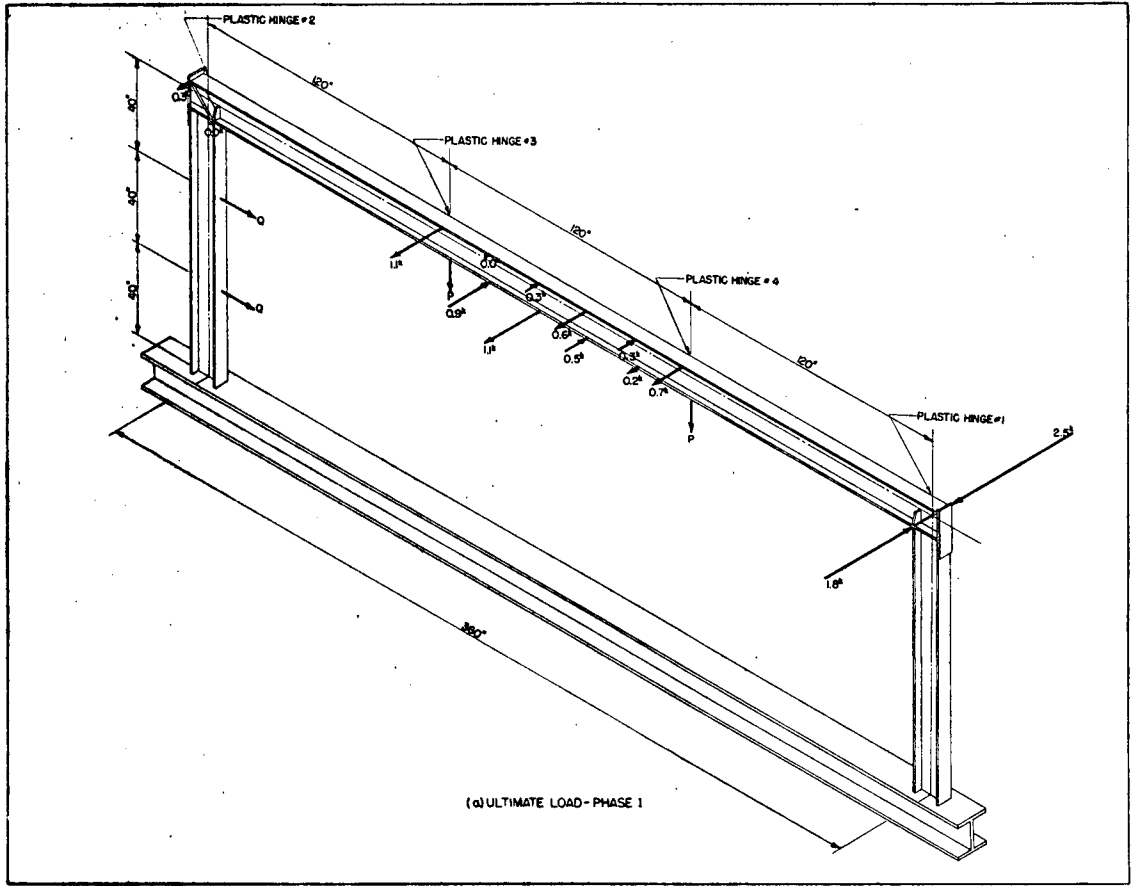


FIG 25 LATERAL SUPPORT FORCES IN FRAME 3



4010-1A



4010-1B

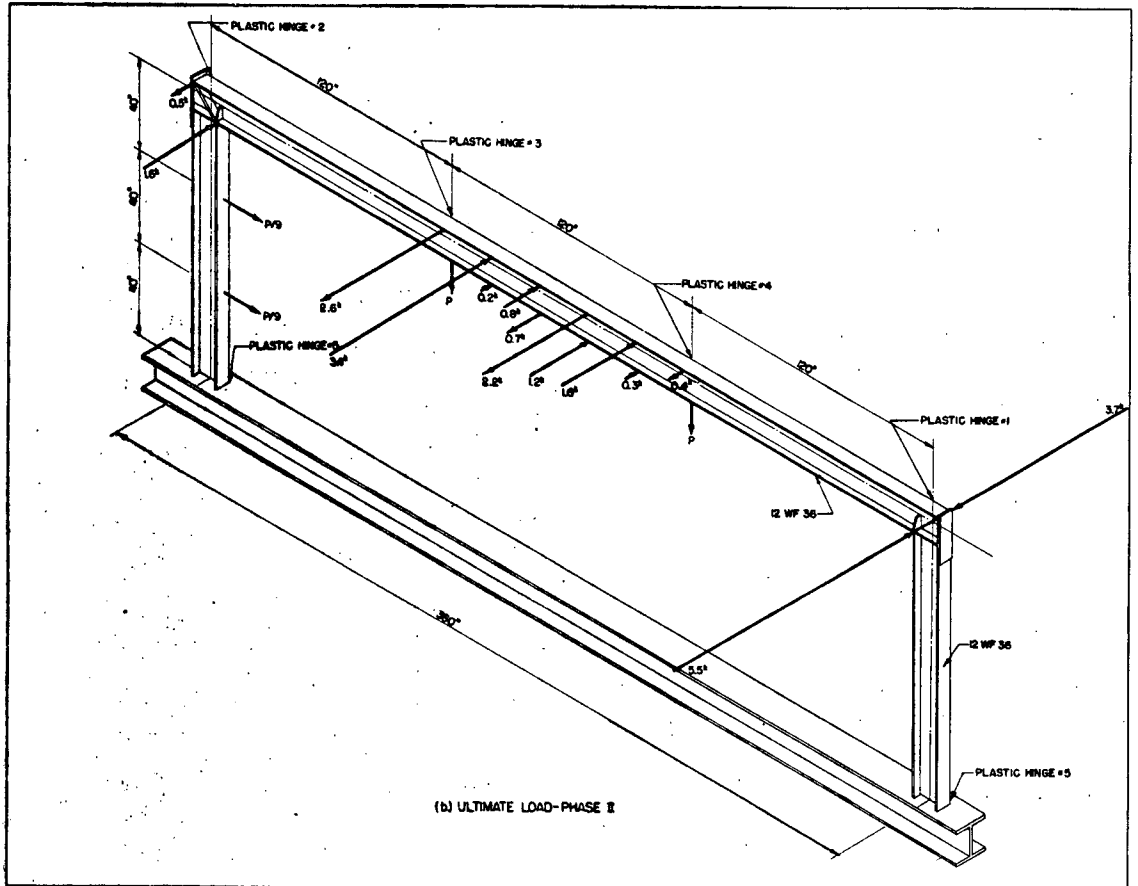


FIG 30 FRAME 4